REMARKS/ARGUMENTS

Objection to the Specification under 35 U.S.C. Section 132:

There was an objection to the prior amendment of the Applicant's patent specification under 35 U.S.C. Section 132. The Applicant respectfully argues that substitution of the term "antennapedia peptides" for the previously used Trademark name of PENETRATIN® does not introduce any new matter. First, PENETRATIN® is the trademark used by Cyclacel Ltd (Dundee, Scotland) for marketing antennapedia peptide. The current United States Patent Office recitation of the goods and services description of PENETRATIN® reads: "Chemical preparations, namely **antennapedia peptide** for pharmaceutical and medical use; pharmaceutical preparations and substances, namely **antennapedia peptide**." (See Appendix A).

Secondly, the term "penetratin" is widely used in both past and current scientific literature to describe the antennapedia peptide. For example, Bart Christiaens et al. in "*Tryptophan Fluoresence Study of the Intercation of Penetratin Peptides with Model Membranes*," European Journal of Biochemistry, Volume 269, Pages 2918-2926, February 2002 states: "**Penetratin** is a 16-residue **peptide** [RQIKIWFQNRRMKWKK(43-58)] derived from the **Antennapedia** homeodomain, which is used as a vector for cellular internalization of hydrophilic molecules." (See Appendix B).

The equivalence of the term penetratin and antennapedia peptide was also widely recognized at the time that the initial application was filed as demonstrated by the statement "Peptides derived from the third alpha-helix of the homeodomain (residues 43-58; Penetratin) of

Antennapedia, a Drosophila homeoprotein, were prepared by simultaneous multiple synthesis" found in Fischer, P.M., Zhelev, N.Z., Wang, S., Melville, J.E., Fåhraeus, R., and Lane, D.P., "*Structure-Activity Relationship of Truncated and Substituted Analogues of the Intracellular Delivery Vector Penetratin*," Journal of Peptide Research, February 2000, Volume 55(2), Pages163-72. (See Appendix C).

The Fischer et al. Reference also demonstrates that use of the term "antennapedia peptides" (plural) as a substitute for the trademark term PENETRATIN® is appropriate as it demonstrates that substitution of hydrophobic residues in the PENETRATIN® peptide sequence does not substantively impact the biological function. Those skilled in the art would readily appreciate that a variety of peptide sequences derived from the native antennapedia or penetratin sequence [RQIKIWFQNRRMKWKK] can deliver substantially equivalent cellular internalization activity. United States Patent Number 5,888,762, which claims the penetratin sequences, also clearly indicates that a number of derivatives of this sequence are expected to have biological activity. (See Appendix D).

In response to the Examiner's query regarding if there are other antennapedia peptides found in the art, when the term "antennapedia peptides" is searched as a term in the field "goods and services" under the Trademark Electronic Search System (TESS) for the United States Trademark Office (See Appendix E), the only federal trademark registration or trademark application that appears is the previously referenced PENETRATIN® as shown in Appendix A.

Therefore, the Applicant now uses the term "antennapedia peptides," which is the exact name of the material sold under the trademark PENETRATIN®. The reference to the trademark was eliminated in the claims to avoid the problems described in the Manual for Patent Examining Procedure that recites: "**The formula or characteristics of the product may change from time to time and yet it may continue to be sold under the same trademark.**" (Manual of Patent Examining Procedure (MPEP) Section 608.01(v)). The Specification was amended in a likewise manner and refers to PENETRATIN® as an example of a source for antennapedia peptides and then describes the name and address of the Entity supplying this material.

It is respectfully believed that a person of ordinary skill in the art would consider PENETRATIN® and antennapedia peptides being synonymous with each term being neither broader nor narrower than the other. Therefore, reference to antennapedia peptides as well as the trademarked term, i.e., PENETRATIN®, simply overcomes the concerns of the United States Patent Office, expressed in the Manual for Patent Examining Procedure, that some other material may someday be sold under this federally registered trademark rather than antennapedia peptides.

Therefore, it is respectfully believed that the rejection under 35 U.S.C. Section 132 is overcome.

Rejection under 35 U.S.C. Section 112:

Claims 22 and 25 were rejected under 35 U.S.C. Section 112, first paragraph, for failing to comply with the written description requirement. In particular, it is alleged that these Claims contain subject matter that was not described in the Specification to reasonably convey to one skilled in the relevant art, at the time the application was filed, possession of the claimed invention. This is deemed a "new matter rejection."

As described previously above, the term "penetratin" is widely used in both past and current scientific literature to describe the antennapedia peptide. (See Appendix B). The equivalence of the term penetratin and antennapedia peptide was also widely recognized at the time that the initial application was filed. (See Appendix C). Moreover, that use of the term "antennapedia peptides" (plural) as a substitute for the trademark term PENETRATIN® is appropriate as it demonstrates that substitution of hydrophobic residues in the penetratin peptide sequence does not substantively impact the biological function. Those skilled in the art would readily appreciate that a variety of peptide sequences derived from the native antennapedia or penetratin sequence [RQIKIWFQNRRMKWKK] can deliver substantially equivalent cellular internalization activity.

In response to the Examiner's query regarding if there are other antennapedia peptides found in the art, when the term "antennapedia peptides" is searched as a term in the field "goods and services" under the Trademark Electronic Search System (TESS) for the United States

Trademark Office (See Appendix E), the only federal trademark registration or trademark application that appears is the previously referenced PENETRATIN® as shown in Appendix A.

Therefore, the Applicant now uses the term "antennapedia peptides," which is the exact name of the material sold under the trademark PENETRATIN®. The reference to the trademark was eliminated in the claims to avoid the problems described in Manual for Patent Examining Procedure that recites: "**The formula or characteristics of the product may change from time to time and yet it may continue to be sold under the same trademark.**" (Manual of Patent Examining Procedure (MPEP) Section 608.01(v)).

It is respectfully believed that a person of ordinary skill in the art would consider PENETRATIN® and antennapedia peptides being synonymous with each term being neither broader nor narrower than the other. Therefore, reference to antennapedia peptides rather than the trademarked term, i.e., PENETRATIN®, simply overcomes the concerns of the United States Patent Office, expressed in the Manual for Patent Examining Procedure, that some other material may someday be sold under this federally registered trademark rather than antennapedia peptides.

Therefore, it is now believed that all of the pending Claims 22 and 25 in the present application are in condition for allowance. Favorable action and allowance of Claims 22 and 25 is therefore respectfully requested. If any issue regarding the allowability of Claims 22 and 25 in the present application could be readily resolved, or if other action could be taken to further advance this application such as an Examiner's amendment, or if the Examiner should have any questions regarding the present amendment, it is respectfully requested that the Examiner please telephone Applicants' undersigned attorney in this regard.

Respectfully submitted,

Dated: August 23, 2004

Kevin M. Kercher
Registration No. 33,408
Blackwell Sanders Peper Martin LLP
720 Olive Street, 24th Floor
St. Louis, Missouri 63101
(314) 345-6000
ATTORNEY FOR APPLICANTS

UNITED STATES PATENT AND TRADEMARK OFFICE

Home | Index | Search | System Alerts | eBusiness Center | News & Notices | Contact Us

APPENDIX A

Trademark Electronic Search System(Tess)

TESS was last updated on Tue Aug 3 04:38:33 EDT 2004

PTO Home | Trademark | TESS Home | New User | Structured | Free Form | Browse Dict | Bottom | Help

Logout Please logout when you are done to release system resources allocated for you.

Record 1 out of 1

Check Status *(TARR contains current status, correspondence address and attorney of record for this mark. Use the "Back" button of the Internet Browser to return to TESS)*

Typed Drawing

Word Mark	**PENETRATIN**
Goods and Services	IC 005. US 006 018 044 046 051 052. G & S: Chemical preparations, namely antennapedia peptide for pharmaceutical and medical use; pharmaceutical preparations and substances, namely antennapedia peptide
Mark Drawing Code	(1) TYPED DRAWING
Serial Number	75452568
Filing Date	March 18, 1998
Current Filing Basis	44E
Original Filing Basis	1B;44D
Published for Opposition	April 9, 2002
Registration Number	2587029
Registration Date	July 2, 2002
Owner	(REGISTRANT) Cyclacel Limited CORPORATION UNITED KINGDOM 5 Whitehall Crescent Dundee, Scotland DD1 4AR UNITED KINGDOM
Attorney of Record	BRUCE S LONDA
Priority Date	February 17, 1998
Type of Mark	TRADEMARK
Register	PRINCIPAL
Live/Dead Indicator	LIVE

PTO Home | Trademark | TESS Home | New User | Structured | Free Form | Browse Dict | Top | Help

Eur. J. Biochem. 269, 2918–2926 (2002) © FEBS 2002 doi:10.1046/j.1432-1033.2002.02963.x

APPENDIX B

Tryptophan fluorescence study of the interaction of penetratin peptides with model membranes

Bart Christiaens[1], Sofie Symoens[1], Stefan Vanderheyden[2], Yves Engelborghs[2], Alain Joliot[3], Alain Prochiantz[3], Joël Vandekerckhove[4], Maryvonne Rosseneu[1] and Berlinda Vanloo[1]

[1]*Laboratory for Lipoprotein Chemistry and* [4]*Flanders Interuniversity Institute for Biotechnology, Department of Medical Protein Research, Faculty of Medicine, Department of Biochemistry, Ghent University, Belgium;* [2]*Laboratory of Biomolecular Dynamics, Katholieke Universiteit Leuven, Belgium;* [3]*Ecole Normale Supérieure, Paris, France*

Penetratin is a 16-amino-acid peptide, derived from the homeodomain of antennapedia, a *Drosophila* transcription factor, which can be used as a vector for the intracellular delivery of peptides or oligonucleotides. To study the relative importance of the Trp residues in the wild-type penetratin peptide (RQIKIWFQNRRMKWKK) two analogues, the W48F (RQIKIFFQNRRMKWKK) and the W56F (RQIKIWFQNRRMKFKK) variant peptides were synthesized. Binding of the three peptide variants to different lipid vesicles was investigated by fluorescence. Intrinsic Trp fluorescence emission showed a decrease in quantum yield and a blue shift of the maximal emission wavelength upon interaction of the peptides with negatively charged phosphatidylserine, while no changes were recorded with neutral phosphatidylcholine vesicles. Upon binding to phosphatidylcholine vesicles containing 20% (w/w) phosphatidylserine the fluorescence blue shift induced by the W56F-penetratin variant was larger than for the W48F-penetratin. Incorporation of cholesterol into the negatively charged lipid bilayer significantly decreased the binding affinity of the peptides. The Trp mean lifetime of the three peptides decreased upon binding to negatively charged phospholipids, and the Trp residues were shielded from acrylamide and iodide quenching. CD measurements indicated that the peptides are random in buffer, and become α helical upon association with negatively charged mixed phosphatidylcholine/phosphatidylserine vesicles, but not with phosphatidylcholine vesicles. These data show that wild-type penetratin and the two analogues interact with negatively charged phospholipids, and that this is accompanied by a conformational change from random to α helical structure, and a deeper insertion of W48 compared to W56, into the lipid bilayer.

Keywords: penetratin; homeoproteins; lipid vesicles; Trp fluorescence; circular dichroism.

Homeoproteins are transcription factors, first discovered in *Drosophila melanogaster*, which are involved in multiple morphological processes [1]. A 60-residue DNA-binding domain, named homeodomain, which consists of three α helices and one β turn between helices 2 and 3 was identified in these proteins [2]. The homeodomain of antennapedia (a *Drosophila* homeoprotein) was shown to translocate through the plasma membrane of cultured neuronal cells, to reach the nucleus and to induce changes in the cellular morphology [3,4]. It was recently shown that the translocation properties of helix 3 are similar to those of the entire homeodomain [5]. Prochiantz *et al.* [6–8] proposed to use the penetratin peptide, corresponding to residues 43–58 of the homeodomain, as a vehicle for the intracellular delivery of hydrophilic cargo molecules [e.g. oligopeptides [9], oligonucleotides [10] and peptidic nucleic acids (PNA) [11]]. The mechanism for the peptide translocation through the cellular membrane remains unclear. Chemical modifications of the penetratin peptide have shown that translocation does not require interactions with chiral receptors or enzymes [12]. The two Trp residues at position 48 and 56 play a crucial role in the translocation process, as a variant peptide with two Trp → Phe substitutions is not internalized [5], suggesting that internalization does not depend only upon the peptide hydrophobicity. Peptide translocation could be explained by formation of inverted micelles, which is promoted by Trp residues [13]. ^{31}P-NMR spectroscopy data showed that addition of penetratin to a lipid extract from embryonic rat brain induced formation of inverted micelles, whereas this was not observed with synthetic lipid membranes [14]. Formation of inverted micelles could also account for the limitation in the length of the cargo that can be internalized after attachment to the penetratin peptide. It is unlikely that penetratin would adopt an α helical conformation leading to formation of a positively charged channel, as the 16-residue peptide is too short to span the plasma membrane. Derossi *et al.* could not measure any conductivity that would support channel formation [12]. The WT-penetratin peptide adopts an α helical structure in 30% (v/v) hexafluoroisopropanol, in perfluoro-*tert*-butanol and in the presence of SDS micelles [14]. However the peptide

Correspondence to B. Vanloo, Department Biochemistry, Laboratory Lipoprotein Chemistry, Ghent University, Hospitaalstraat 13, 9000 Ghent, Belgium.
Fax: + 32 9264 94 96, Tel.: + 32 9264 92 73,
E-mail: berlinda.vanloo@rug.ac.be

Abbreviations: PtdCho, egg yolk phosphatidylcholine; PtdSer, bovine brain phosphatidylserine; PamOle-PtdGro, 1-palmitoyl-2-oleoylphosphatidyl-DL-glycerol; TFE, 2,2,2-trifluoroethanol; SUV, small unilamellar vesicle.

(Received 2 January 2002, revised 19 April 2002, accepted 25 April 2002)

α helicity is not required for internalization, as introduction of one or three prolines in the sequence, did not affect peptide internalization [12].

The aim of this study was to gain better insight into the mode of interaction of the penetratin peptide with lipid bilayers and to investigate the role of the Trp residues and the lipids in this interaction. Lipid–peptide interactions can conveniently be monitored through changes in Trp fluorescence emission properties of the peptide upon interaction with model membranes [15–17]. For this purpose, two penetratin analogues, in which Trp48 and Trp56 were substituted by a phenylalanine, were synthesized. We studied the interaction of the WT-penetratin and the two W48F- and W56F-variants, with sonicated lipid vesicles, consisting either of zwitterionic phosphatidylcholine (PtdCho) or of a mixture of PtdCho with negatively charged phosphatidylcholine (PtdSer). We further investigated the effect of cholesterol incorporation into lipid bilayers containing negatively charged phospholipids. Fluorescence lifetime measurements yielded the lifetimes of the Trp residues in lipid-free and lipid-bound peptides. Acrylamide and iodide quenching of Trp fluorescence, enabled probing of the accessibility of the Trp residues. Changes in the α helical conformation upon lipid binding were investigated by CD measurements.

EXPERIMENTAL PROCEDURES

Materials

Egg PtdCho, bovine brain PtdSer, cholesterol and 2,2,2-trifluoroethanol (TFE) were purchased from Sigma Chemical Co. The *N*-α-Fmoc amino acids and reagents for peptide synthesis and sequencing were purchased from Novabiochem and Sigma Chemical Co.

Peptide synthesis

Peptides were synthesized using the Fmoc-tBU strategy on an AMS 422 peptide synthesizer (ABIMED, Germany) by Synt:em (Nimes, France). The peptides were cleaved from the resin by trifluoroacetic acid (90%) and purified by RP-HPLC using various acetonitrile gradients in aqueous 0.1% trifluoracetic acid. The purity was more than 95%. Peptide molecular masses were determined by MALDI-TOF mass spectrometry (Perspective Biosystem, UK). Peptides were lyophilized and weighed, and 1 $mg{\cdot}mL^{-1}$ solutions were prepared in a 10 mM Tris/HCl buffer, pH 8.0, 0.15 M NaCl, 3 mM EDTA, 1 mM NaN_3. Exact concentration was determined by Phe quantification and by absorbance measurements at 280 nm using molar extinction coefficients of 11 400 and 6000 $M^{-1}{\cdot}cm^{-1}$, respectively, for WT-penetratin and for the two analogues.

Small unilamellar vesicle (SUV) preparation

Lipids were dissolved in chloroform and dried as a thin film, first under nitrogen followed by vacuum for 3 h. Lipid suspension was prepared by vortex mixing in a 10 mM Tris/HCl buffer, pH 8.0, 0.15 M NaCl, 3 mM EDTA, 1 mM NaN_3. The suspension was sonicated at 4 °C, under nitrogen for 30 min using a Sonics Material Vibra-Cell™ sonicator. Titanium debris was removed by centrifugation. SUVs were separated from multilamellar vesicles by gel filtration on a Sepharose CL 4B column. The top fractions of the SUV peak were pooled, concentrated and stored at 4 °C. Phospholipid and cholesterol concentrations were determined by enzymatic colorimetric assays (bioMérieux, France; Boehringer, Germany); total lipid concentration was determined by phosphorus analysis [18].

Fluorescence titration measurements

Peptide–phospholipid interactions were studied by monitoring the changes in the Trp fluorescence emission spectra of the peptides upon addition of SUVs. Intrinsic fluorescence of the Trp residues of the penetratin peptides was measured before and after addition of different amounts of phospholipid vesicles to a 2 μM peptide solution. Trp fluorescence was measured at 25 °C in an Aminco Bowman Series 2 spectrofluorometer, equipped with a thermostatically controlled cuvette holder after mixing. Emission spectra were recorded between 310 and 450 nm with an excitation wavelength of 280 nm, at slit widths of 4 nm. Correction for light scattering was carried out by subtracting the corresponding spectra of the SUVs.

Peptide–lipid binding was determined from the quenching of the intrinsic Trp fluorescence intensity of the peptides, upon addition of SUVs. The fluorescence intensity at 350 nm, expressed as the percentage of the fluorescence of the lipid-free peptide was plotted vs. the added lipid concentration. The data were analyzed using SIGMAPLOT (SPSS Inc.).

The change in the fluorescence of the peptide can be described by the following equation:

$$F = (F_0[P_F] + F_1[PL])/([P_F] + [PL]) \quad (1)$$

where F is the fluorescence intensity at a given added lipid concentration, F_0 the fluorescence intensity at the beginning of the titration, F_1 the fluorescence intensity at the end of the titration, $[P_F]$ the concentration of free peptide and [PL] the concentration of the peptide–lipid complex.

The concentration of PL can be obtained via the definition of the dissociation (association) constant:

$$K_d = 1/K_a = ([P_F][L_F])/[PL] \quad (2)$$

with K_d dissociation constant, K_a association constant, $[P_F]$ free peptide concentration, $[L_F]$ free lipid concentration and [PL] peptide–lipid complex concentration.

For low affinity associations one can assume that after lipid addition, the free lipid concentration $[L_F]$ equals the total lipid concentration $[L_{tot}]$. Eqn (2) can be written as:

$$[PL] = K_a[L_{tot}][P_F] \quad (3)$$

Substitution of Eqn (3) in Eqn (1) leads to:

$$F = (F_0 + F_1K_a[L_{tot}])/(1 + K_a[L_{tot}]) \quad (4)$$

K_a can thus be determined by plotting the measured fluorescence intensity (F) as a function of the total concentration lipid added.

For high affinity associations the binding Eqn (2) was rearranged to the following quadratic equation:

$$[PL]^2 - [PL]([P_{tot}] + [L_{tot}]/n + K'_d) + ([L_{tot}]/n)[P_{tot}] = 0 \quad (5)$$

The parameter n, representing the formal number of phospholipid molecules that are involved in a binding site for one peptide, is introduced in order to account for the formal stoichiometry of binding ($K_d' = K_d/n$). The solution of this quadratic equation is thus given by:

$$[PL] = \{S \pm (S^2 - 4([L_{tot}]/n)[P_{tot}])^{1/2}\}/2 \quad (6)$$

with

$$S = [P_{tot}] + [L_{tot}]/n + K'_d$$

Substitution of Eqn (6) into Eqn (1) yields an equation of F as a function of $[P_{tot}]$ and $[L_{tot}]$. By plotting the measured fluorescence intensity as a function of $[L_{tot}]$, K'_d and n can be determined. K_d is obtained by multiplying of K'_d by n.

Fluorescence lifetime measurements

Fluorescence lifetimes were determined using an automated multifrequency phase fluorimeter. The instrument is similar to that described by Lakowicz *et al.* [19], except for the use of a high-gain photomultiplier (Hamamatsu H5023) instead of a microchannel plate. The excitation source consists of a mode-locked, titanium-doped sapphire laser (Tsunami; Spectra Physics) pumped by a Beamlok 2080 Ar^+-ion laser (2080; Spectra Physics) and equipped with a pulse selector (Spectra Physics model 3980) to reduce the basic repetition frequency to 0.4 MHz. After frequency tripling (frequency tripler Spectra Physics model GWU), the excitation wavelength is 295 nm. The detection system was described previously by Vos *et al.* [20]. In this way, fluorescence lifetime measurements were performed by measuring the phase shift of the modulated emission at 50 frequencies ranging from 0.4 MHz to ≈1 GHz. *N*-Acetyl-L-typtophanamide (in water at 21 °C), with a lifetime of 3.12 ns, was used as a reference fluorophore. The measured phase shifts (ϕ) at a modulation frequency (ω) of the exciting light are related to the fluorescence decay in the time domain as described previously. Data analysis was performed as described by De Beuckeleer *et al.* [21].

Quenching experiments

Peptide–lipid interactions are accompanied by changes in the accessibility of the peptides to aqueous quenchers of Trp fluorescence upon addition of SUVs. Acrylamide [22] and iodide [23] quenching experiments were carried out on a 2 μM peptide solution in the absence or presence of SUVs by addition of aliquots of 2 M acrylamide solution or a 2 M potassium iodide solution (containing 1 mM $Na_2S_2O_3$ to prevent I_3^- formation). The lipid–peptide mixtures (molar ratio of 50 : 1) were incubated for 1 h at room temperature prior to the measurements. The excitation wavelength was set at 295 nm instead of 280 nm to reduce the absorbance by acrylamide and iodide. Fluorescence intensities were measured at 350 nm after addition of quencher at 25 °C. The quenching constants were obtained from the slope of the Stern–Volmer plots of F_0/F vs. [quencher], with F_0 and F the fluorescence intensities in the absence and presence of quencher, respectively.

Circular dichroism measurements

CD measurements were carried out at room temperature on a Jasco 710 spectropolarimeter between 184 and 260 nm in quartz cells with a path length of 0.1 cm. Nine spectra were recorded and averaged. The peptides were dissolved at a concentration of 50 $\mu g \cdot mL^{-1}$ in a 10 mM sodium phosphate buffer and in 20, 50 and 100% TFE. CD spectra of the lipid bound peptides were recorded after 1 h incubation at room temperature of the peptides with the liposomes at a molar ratio of 1 : 20 or 1 : 40. The spectra were corrected for minor contributions of the SUVs by subtracting the measured spectra of the lipids alone. The secondary structure of the peptides was determined by curve fitting to reference protein spectra using the CDNN program [24]. The helicity of the peptides was determined from the mean residue ellipticity [Θ] at 222 nm [25].

RESULTS

The sequences of the WT and variant peptides, with a Trp → Phe substitution at position 48 and 56 are RQIKIWFQNRRMKWKK, RQIKIFFQNRRMKWKK and RQIKIWFQNRRMKFKK, respectively. These substitutions did not affect the mean hydrophobicity, which was −0.61, −0.58 and −0.58, respectively [26].

Binding of the penetratin peptides with lipid vesicles

Peptide binding to lipid vesicles was investigated by intrinsic Trp fluorescence emission measurements. WT and variant peptides were incubated with lipid vesicles consisting of either pure PtdCho, PtdCho/PtdSer at different weight ratios, or pure PtdSer (Table 1). 10% cholesterol was also included in the PtdCho/PtdSer mixed vesicles.

The Trp fluorescence emission spectra of the WT-penetratin peptide, measured either in buffer or in the presence of lipid vesicles are shown on Fig. 1. The maximal emission wavelength (λ_{max}) was ≈347 nm in buffer, as previously reported for Trp in an aqueous environment [27]. Addition of PtdCho vesicles did not affect the shape of the Trp fluorescence spectrum and only slightly decreased the intensity (Fig. 1). On the contrary, addition of mixed PtdCho/PtdSer vesicles containing 10 and 20% negatively charged PtdSer, shifted λ_{max} to lower wavelengths and decreased significantly the intensity. This blue shift, indicative of a more hydrophobic environment of the Trp residues, increased from 2 to 12 nm for PtdCho/PtdSer vesicles with 10 and 20% PtdSer, respectively. Incorporation of 10% cholesterol in mixed PtdCho/PtdSer vesicles had a similar effect on λ_{max}. Incubation of the peptide with pure PtdSer vesicles decreased λ_{max} by 11 nm. Similar spectra were obtained with the W48F- and W56F-penetratin peptides. When incubated with mixed PtdCho/PtdSer vesicles with 20% PtdSer, λ_{max} and $\Delta\lambda$ of the W56F variant differed more from the WT peptide than the values of the W48F variant (Table 1). λ_{max} values for the lipid-bound peptides were 337.5 and 334.5 nm for the W48F- and W56F-penetratin, respectively, compared to 336 nm for WT-penetratin; a larger blue shift of 12.5 nm was measured for the W56F variant compared to 9.5 nm for the W48F variant.

The corresponding titration curves obtained for the WT peptide by plotting the percentage of initial fluorescence as a

Table 1. Maximal Trp emission wavelength (λ_{max}), dissociation constants (K_d) and binding stoichiometry (n, mole lipid/mole peptide) for the binding of the penetratin peptides with different lipid vesicles. *n* is determined for high affinity binding curves. ND, not determined; chol, cholesterol. SD = 0.5 nm, number of experiments = 3.

		WT-penetratin			W48F-penetratin			W56F-penetratin		
Lipid	Lipid ratio (%, w/w)	λ_{max} (nm)	K_d (μM)	*n*	λ_{max} (nm)	K_d (μM)	*n*	λ_{max} (nm)	K_d (μM)	*n*
Peptide	–	347.0	–	–	347.0	–	–	347.0	–	–
+ PtdCho	100	347.0	230	ND	347.0	350	ND	347.0	320	ND
+ PtdCho/PtdSer	90 : 10	345.0	137 ± 19	ND	345.5	102 ± 16	ND	345.0	103 ± 33	ND
+ PtdCho/PtdSer	80 : 20	336.0	0.67 ± 0.19	13	337.5	8.5 ± 3.9	12	334.5	0.99 ± 0.30	17
+ PtdSer	100	336.5	0.37 ± 0.09	11	336.0	1.1 ± 0.4	9	337.0	0.63 ± 0.39	5
+ PtdCho/PtdSer/chol	70 : 20 : 10	339.0	44 ± 4.4	ND	341.0	114 ± 14	ND	338.5	86 ± 17	ND

function of the lipid concentration are shown in Fig. 2. Incubation of WT with pure PtdCho vesicles had little effect on the Trp fluorescence intensity of the peptides (Fig. 2), suggesting a low affinity of the peptide for this zwitterionic phospholipid. Incorporation of negatively charged PtdSer into the PtdCho vesicles significantly decreased the Trp fluorescence intensity for the WT peptide. The Trp fluorescence intensity titration curves show saturable binding of the WT-penetratin peptide to mixed PtdCho/PtdSer vesicles containing 20% PtdSer or to pure PtdSer vesicles. Similar titration curves were obtained for the W48F and W56F penetratin peptides. Apparent dissociation constants, K_d, were determined by curve fitting (Table 1). Interaction of the peptides with PtdCho vesicles and with mixed PtdCho/PtdSer vesicles containing 10% PtdSer was weak, as K_d values were around 230–350 and 100–140 μM, respectively. For the mixed PtdCho/PtdSer vesicles containing 20% PtdSer and the 100% PtdSer vesicles, the dissociation constant decreased by one or two orders of magnitude. The K_d was around 1 μM for pure PtdSer vesicles. For lipid vesicles containing 20% PtdSer, K_d values were highest for the W48F variant (8.5 μM) while the WT- and W56F-penetratin peptide had similar affinity (0.67 and 0.99 μM, respectively). Incorporation of 10% cholesterol into the PtdCho/PtdSer vesicles at a 70 : 20 : 10 (w/w/w) ratio increased the dissociation constant 10- to 20-fold for each peptide, compared to the corresponding 20% PtdSer vesicles (Table 1). We also observed a decrease in the blue shift upon addition of 10% cholesterol to the 20% PtdSer vesicles. The stoichiometry (*n*) for lipid/peptide association was calculated for the high affinity binding curves to mixed PtdCho/PtdSer and PtdSer vesicles. It varied between 5 and 17 mol lipid per mol peptide, and was similar for the three peptides (Table 1).

The effect of salt concentration on the binding affinity of WT-penetratin to PtdCho/PtdSer vesicles containing 20% PtdSer was investigated. The dissociation constant increased by one to two orders of magnitude in buffers containing, respectively, 0.5 and 1 M NaCl. The accompanying blue shift was limited to 1–3 nm at high salt concentration (data not shown), suggesting a significant role for electrostatic interactions in lipid–peptide binding.

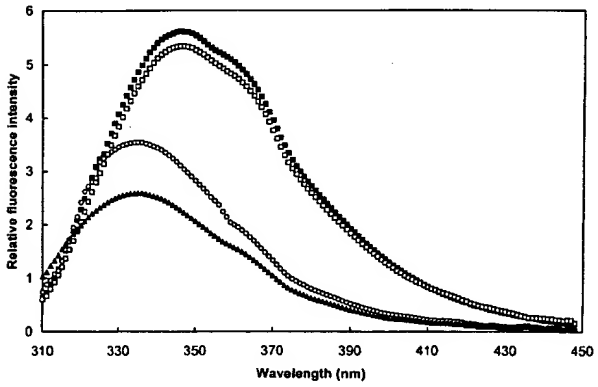

Fig. 1. Fluorescence emission spectra of WT-penetratin in buffer (■), in the presence of PtdCho vesicles (□), of mixed PtdCho/PtdSer vesicles at a 80 : 20, w/w ratio (○), and of PtdSer vesicles (▲). Peptide and lipid concentration were, respectively, 2 μM and 100 μM.

Fluorescence lifetimes

The fluorescence decay parameters of the Trp residue(s) for the three penetratin peptides were determined at pH 8, in

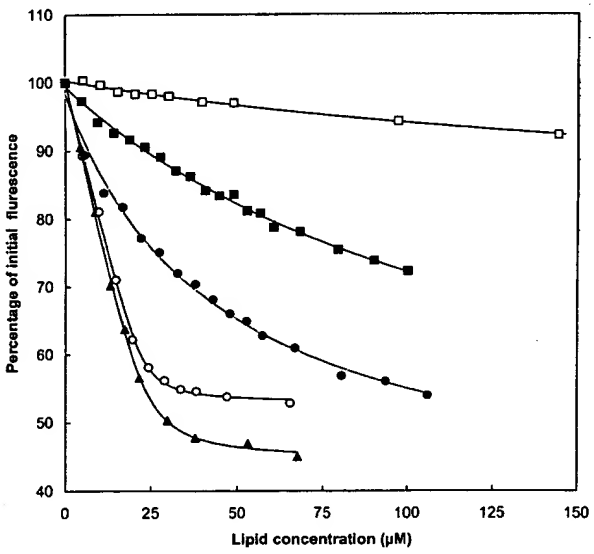

Fig. 2. Fluorescence titration curves of WT-penetratin with lipid vesicles consisting of PtdCho (□), PtdCho/PtdSer (90 : 10, w/w) (■), PtdCho/PtdSer (80 : 20, w/w) (○), PtdSer (▲) and PtdCho/PtdSer/chol (70 : 20 : 10, w/w/w) (●). The solid lines represents the best fits to the binding curves.

the absence and presence of PtdCho/PtdSer (20 : 80, w/w) vesicles. The fluorescence curves could be optimally fitted using a triple-exponential decay, even at relatively high χ^2_R values. The amplitudes and lifetimes, together with the calculated mean lifetime $\langle\tau\rangle$ for the Trp residue(s) of the three peptides, are summarized in Table 2. Mean lifetimes of, respectively, 2.25, 2.06 and 2.45 ns were obtained for the WT-, W48F- and W56F-penetratin in buffer. Upon addition of the mixed PtdCho/PtdSer vesicles containing 80% PtdSer at a molar lipid/peptide ratio of 25 : 1, the shortest lifetime components τ_1 and τ_2 decreased strongly, while the longest lifetime component τ_3 of the Trp residue in the W48F-penetratin increased slightly. The amplitude of the longest Trp lifetime component decreased 10-fold whereas the amplitude of the shortest lifetime component increased threefold for all three peptides. This resulted in, respectively, a sevenfold and a fourfold to fivefold decrease of the mean lifetime of the Trp residue(s) in the W56F- and WT- or W48F-penetratin. The decrease of the mean Trp lifetime for the three peptides might account for the decrease of the Trp fluorescence intensity upon binding to negatively charged lipid vesicles. Increasing the amount of added lipid to a 50 : 1 molar ratio did not further decrease the mean lifetimes.

The lifetimes of the WT-, W48F- and the W56F-penetratin were further measured in TFE, a decrease of the mean lifetime was observed for all peptides (Table 2).

Acrylamide and iodide quenching of lipid-free and lipid-bound penetratin peptides

Fluorescence quenching by acrylamide and iodide was used to monitor the Trp environment of the lipid-free and lipid-bound peptides. It was compared to the quenching of free Trp in a Tris/HCl buffer and in the presence of lipids. Stern–Volmer plots of acrylamide (A) and iodide (B) quenching are shown in Fig. 3 for WT-penetratin in buffer and in the presence of PtdCho, mixed PtdCho/PtdSer vesicles and PtdSer vesicles. The calculated Stern–Volmer constants (K_{sv}) are summarized in Table 3. Acrylamide quenching (Fig. 3A) was efficient in the Tris/HCl buffer, as K_{sv} for the three peptides amounted up to 70% of that of Trp. Incubation with neutral PtdCho vesicles had no effect on acrylamide quenching, while addition of mixed PtdCho/PtdSer or of pure PtdSer vesicles significantly decreased the K_{sv} values for the three peptides. A twofold decrease of K_{sv} was observed for PtdCho/PtdSer vesicles containing 10% PtdSer up to a sixfold to sevenfold decrease for pure PtdSer vesicles. Incorporation of cholesterol into PtdCho/PtdSer vesicles (PtdCho/PtdSer/cholesterol 70 : 20 : 10, w/w/w) decreased the acrylamide quenching to a similar extent as for the corresponding PtdCho/PtdSer (80 : 20, w/w) vesicles. Similar results were obtained for iodide quenching (Fig. 3B, Table 3). For the lipid-free peptides, we calculated the average rate constant for collisional quenching, from the Stern–Volmer constant using the average lifetime ($k_q = K_{SV}/\langle\tau\rangle$). For acrylamide quenching, k_q values were, respectively, 6.2, 6.1 and 5.9×10^9 $M^{-1}\cdot s^{-1}$ for WT-, W48F- and W56F-penetratin. These values are similar to the k_q value of 6.6×10^9 $M^{-1}\cdot s^{-1}$ obtained for free Trp. For iodide quenching, k_q values amount to, respectively, 4.9, 5.6 and 4.6×10^9 $M^{-1}\cdot s^{-1}$ for WT-, W48F- and W56F-penetratin. These values are slightly higher than the k_q value measured for free Trp, which amounted up to 3.6×10^9 $M^{-1}\cdot s^{-1}$. Upon addition to the peptides of negatively charged PtdCho/PtdSer vesicles, containing 80% PtdSer, k_q values decreased threefold and fivefold for acrylamide and iodide quenching, respectively, indicating shielding of the Trp residues against collision with the quenchers.

Secondary structure of the lipid-free and lipid-bound peptides

The CD spectra of WT-penetratin in phosphate buffer, after addition of TFE and upon incubation with neutral and anionic vesicles are shown in Fig. 4. The percentages of α helical structure are listed in Table 4. The CD spectrum for the WT peptide in the phosphate buffer is indicative of a predominantly random structure with only a small amount of helix. In the presence of 50% TFE, the shape of the spectrum is that of an α helical structure, with the characteristic minima at 208 and 222 nm. The percentage of α helix increased from ≈ 10% in buffer to 66–72% in 100% TFE. An increase in α helical structure was also observed upon incubation with the anionic mixed PtdCho/PtdSer vesicles

Table 2. Trp fluorescence lifetimes (τ, ns) and amplitudes (a) at 350 nm of the penetratin peptides in the absence and presence of negatively charged PtdCho/PtdSer vesicles (20 : 80, w/w). $\langle\tau\rangle$ is calculated as $\langle\tau\rangle = \Sigma_i a_i\tau_i$.

Peptide	Lipid/peptide molar ratio	τ_1	τ_2	τ_3	a_1	a_2	a_3	$\langle\tau\rangle$	χ^2_R
WT-penetratin	– (buffer)	0.48 ± 0.07	2.15 ± 0.26	4.06 ± 0.22	0.28 ± 0.02	0.44 ± 0.06	0.28 ± 0.04	2.25	1.0
	– (TFE)	0.36 ± 0.10	1.53 ± 0.18	4.28 ± 0.32	0.36 ± 0.05	0.50 ± 0.03	0.14 ± 0.01	1.50	3.8
	25 : 1	0.14 ± 0.01	1.09 ± 0.06	3.43 ± 0.13	0.66 ± 0.02	0.26 ± 0.01	0.081 ± 0.003	0.65	3.5
	50 : 1	0.15 ± 0.01	1.12 ± 0.07	3.46 ± 0.18	0.72 ± 0.02	0.22 ± 0.01	0.060 ± 0.002	0.56	2.9
W48F-penetratin	– (buffer)	0.42 ± 0.09	1.90 ± 0.37	3.40 ± 0.44	0.25 ± 0.03	0.40 ± 0.08	0.35 ± 0.08	2.06	1.7
	– (TFE)	0.36 ± 0.06	1.33 ± 0.10	4.33 ± 0.32	0.38 ± 0.04	0.55 ± 0.03	0.062 ± 0.005	1.15	3.5
	25 : 1	0.10 ± 0.07	1.23 ± 0.23	3.63 ± 0.15	0.82 ± 0.01	0.13 ± 0.04	0.04 ± 0.01	0.40	3.3
	50 : 1	0.14 ± 0.05	1.40 ± 0.14	4.06 ± 0.40	0.78 ± 0.01	0.18 ± 0.01	0.043 ± 0.003	0.53	6.6
W56F-penetratin	– (buffer)	0.52 ± 0.06	1.99 ± 0.28	3.99 ± 0.16	0.28 ± 0.03	0.29 ± 0.03	0.43 ± 0.06	2.45	1.1
	– (TFE)	0.39 ± 0.08	1.76 ± 0.17	4.48 ± 0.36	0.34 ± 0.04	0.51 ± 0.02	0.15 ± 0.01	1.70	3.1
	25 : 1	0.10 ± 0.01	0.85 ± 0.21	2.60 ± 0.13	0.77 ± 0.01	0.18 ± 0.01	0.046 ± 0.002	0.35	2.8
	50 : 1	0.12 ± 0.02	1.04 ± 0.25	3.29 ± 0.27	0.78 ± 0.02	0.18 ± 0.01	0.041 ± 0.002	0.42	6.2

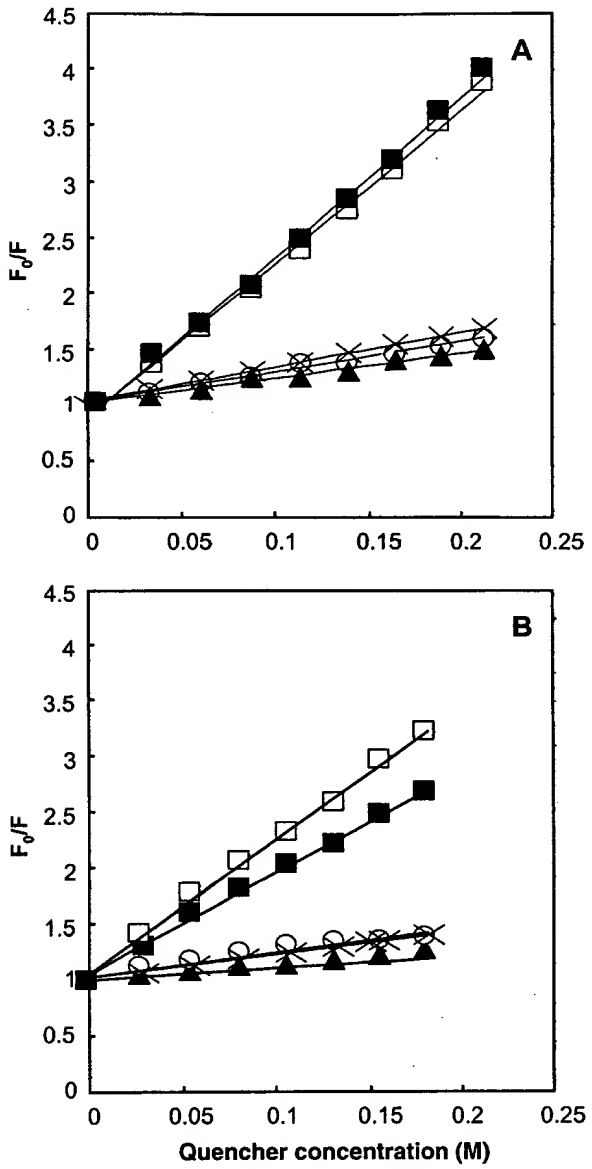

Fig. 3. Stern–Volmer plots for the Trp fluorescence quenching of WT-penetratin in buffer (■), and in the presence of lipid vesicles consisting of PtdCho (□), PtdCho/PtdSer (80 : 20 w/w) (○), PtdSer (▲) and PtdCho/PtdSer/chol (70 : 20 : 10, w/w/w) (×) by the aqueous quenchers acrylamide (A) and iodide (B).

(Fig. 4). Addition of PtdCho vesicles to the WT peptide did not significantly affect the CD spectrum of the peptide compared to that measured in buffer. Similar results were obtained for the W48F-and W56F-penetratin peptides (Table 4).

DISCUSSION

This study was aimed at getting better insight in the interaction of penetratin peptides with lipids, and especially in the contribution of the Trp residues and of negatively charged lipids. We therefore investigated the fluorescence properties of the W48 and W56 residues, either in combination in the WT-penetratin, or separately in the W48F- and the W56F-penetratin single variants, and the effect of incorporating negatively charged PtdSer and cholesterol in the PtdCho vesicles.

In lipid-free penetratin peptides, the two Trp residues are highly exposed to the solvent, and the maximal emission wavelength of 347 nm suggests that WT and penetratin variants are not significantly aggregated in solution. This was confirmed by the extent of acrylamide quenching, which is relatively high compared to other peptides [23,28,29]. In buffer, the peptides and free Trp were quenched by iodide with similar efficiency. A more efficient iodide quenching was also reflected in k_q values higher than for free Trp. This might be due to the electrostatic interaction between positively charged residues of the peptides and negatively iodide ions.

Addition of neutral lipid vesicles to the peptides induced no blue shift of λ_{max} and had little effect on acrylamide and iodide quenching. This suggests only a weak interaction between the peptides and PtdCho vesicles, and a limited insertion of the peptides into the hydrophobic core of the lipid bilayer. These weak interactions are reflected in the high apparent dissociation constants, calculated from the fluorescence titration curves. In contrast, the three peptides strongly interacted with negatively charged lipid vesicles containing 20% (w/w) or more PtdSer, yielding a blue shift of 10–13 nm. The blue shift was more pronounced for the W56F- than for the W48F-penetratin with the mixed PtdCho/PtdSer vesicles containing 20% PtdSer, suggesting a deeper insertion of Trp48 into the lipid bilayer. The lower affinity of the W48F-penetratin variant for lipids, suggested by higher K_d values than for the W56F-penetratin variant further supports the tighter association of Trp48 with lipids.

The interaction with mixed PtdCho/PtdSer or PtdSer vesicles decreased Trp quenching by acrylamide and iodide, as illustrated by the low K_{sv} values and by the lower collision quenching constants. Shielding from iodide quenching by vesicles containing 20% PtdSer or more, was larger for the W56F- than for the W48F-penetratin variant, in agreement with the deeper insertion of Trp48 into the lipids.

According to Lindberg & Graslund, the C-terminus of WT-penetratin inserts deeply into SDS micelles, whereas residues 48–50 are closer to the micellar surface [42]. Size differences between the PtdCho/PtdSer vesicles used in our study, and the smaller SDS micelles with high curvature and full negative charge used by Lindberg & Graslund, might account for the discrepancy between the data. The interaction and orientation of the peptides might indeed be dependent upon the model membrane system used. Drin *et al.* [30] further showed a higher decrease of the binding affinity of 7-nitrobenz-2-oxo-1,3-diazol-4-yl-penetratin peptides for negatively charged 1-palmitoyl-2-oleoylphosphatidyl-DL-choline/1-palmitoyl-2-oleoylphosphatidyl-DL-glycerol (PamOle-PtdGro) vesicles, for the W48A compared to the W56A variant. Deletion of Trp48 and Phe49 in the third helix of antennapedia completely impaired the internalization of the Antp-HD 48S peptide [4]. A penetratin variant, with two Trp → Phe substitutions was internalized to a small extent or not at all [5]. Joliot *et al.* further showed that the engrailed homeoprotein, with an Ile residue at position 56 of its homeodomain, was efficiently internalized [31]. The functional importance of Trp48 is further supported by its higher degree of conservation (> 95%) among the primary

Table 3. Stern–Volmer constants K_{sv} for fluorescence emission quenching of pure Trp and of Trp residues in penetratin peptides before and after incubation with lipid vesicles. Chol, cholesterol; ND, not determined.

		Acrylamide quenching				Iodide quenching			
		Stern–Volmer constant K_{sv} (M^{-1})				Stern–Volmer constant K_{sv} (M^{-1})			
Lipid	Lipid ratio (%, w/w)	Trp	WT-penetratin	W48F-penetratin	W56F-penetratin	Trp	WT-penetratin	W48F-penetratin	W56F-penetratin
–		20.7	14.0	12.6	14.4	11.3	11.1	11.5	11.3
+ PtdCho	100	ND	12.0	12.7	11.1	10.4	13.0	12.0	10.7
+ PtdCho/PtdSer	90 : 10	ND	5.8	7.1	7.2	ND	ND	ND	ND
+ PtdCho/PtdSer	80 : 20	ND	3.0	2.9	4.0	11.5	2.3	2.7	2.2
+ PtdSer	100	ND	3.3	1.9	1.8	11.1	1.1	2.1	1.2
+ PtdCho/PtdSer/chol	70 : 20 : 10	ND	3.1	2.5	2.7	ND	2.2	2.8	2.2

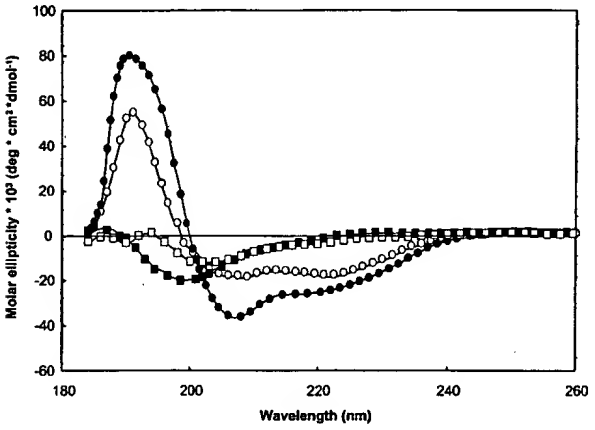

Fig. 4. CD spectra of WT-penetratin in a phosphate buffer, pH 7.4 (■), in 50%TFE (●), in the presence of lipid vesicles consisting of PtdCho (□) and PtdCho/PtdSer (80 : 20, w/w) (○). Peptide concentration was 22 μM, lipid concentration was 880 μM.

sequences of 346 different homeodomains, compared to only 32% conservation for Trp56 [1].

Significant binding of the three peptides was only observed to negatively charged vesicles, suggesting higher contribution of electrostatic compared to hydrophobic interactions, as expected for basic peptides with a pI of 12.6. This is further supported by the 10- to 100-fold increase of the apparent dissociation constants at high salt concentrations. The weak binding observed to mixed PtdCho/PtdSer 90 : 10 vesicles might be due to the low number of negatively charged lipids in the outer bilayer of the vesicles, as the apparent dissociation constant decreased 10- to 100-fold when PtdSer content increased from 10 to 100%. Similar results were reported for the binding of the magainin 2 cationic peptide to PtdCho/PamOle-PtdGro vesicles [32]. The apparent binding constant of magainin 2 increased 10-fold, when the PamOle-PtdGro content increased from 25 to 100%. Addition of cholesterol to PtdCho/PtdSer 80 : 20 vesicles, significantly decreases both the binding affinity and the blue shift, probably due to an increased rigidity of the unsaturated phospholipid acyl chains in the cholesterol-containing vesicles. In spite of the decreased affinity of the penetratin peptides for cholesterol-containing vesicles, the remaining blue shift was still significant. The similar acrylamide and iodide quenching in PtdCho/PtdSer and PtdCho/PtdSer/cholesterol vesicles further support an insertion of the peptides into the core of the bilayer. Similar effects were reported for the interaction of magainin antibacterial peptides to PtdCho/cholesterol vesicles [33]. Calcein leakage induced by the nisin cationic peptide from 1-palmitoyl-2-oleoylphosphatidyl-DL-choline vesicles was further inhibited by formation of liquid-ordered lipid phases in the presence of cholesterol [34].

Insertion of a Trp residue into a more hydrophobic environment is usually characterized by a fluorescence blue shift and by an increase in the fluorescence quantum yield [35]. However, the blue shift for the binding of penetratin

Table 4. Percentages of α helical structure of the lipid-free and lipid-bound penetratin peptides.

		WT-penetratin		W48F-penetratin		W56F-penetratin	
	Lipid/peptide molar ratio	CDNN[a]	$[\Theta]_{222}$[b]	CDNN[a]	$[\Theta]_{222}$[b]	CDNN[a]	$[\Theta]_{222}$[b]
Buffer	–	11	8	8	6	10	9
20% TFE	–	32	26	28	25	35	29
50% TFE	–	62	55	65	59	65	61
100% TFE	–	69	66	72	68	71	67
+ PtdCho	20 : 1	14	13	17	10	11	13
+ PtdCho/PtdSer (80 : 20, w/w)	20 : 1	29	24	21	16	26	22
+ PtdCho/PtdSer (80 : 20, w/w)	40 : 1	42	35	29	25	43	34

[a] Helical content as calculated by curve fitting to reference protein spectra using the CDNN program [24]. [b] Helical content as calculated from $[\Theta]_{222}$ according to Chen *et al.* [25].

peptides to PtdCho/PtdSer vesicles was accompanied by at least a twofold decrease of the fluorescence intensity and a decrease of the mean Trp lifetime, in contrast with the behaviour of other peptides [17]. The three lifetimes of penetratins are attributed to the classical three rotamers of chi1 (Cα–Cβ). The average lifetime of the lipid-free WT-penetratin was calculated from the average lifetimes of the individual Trp residues, assuming pure additivity [20]. This indicates that there are no significant interactions between Trp48 and Trp56, either directly by energy transfer, or indirectly by conformational effects. The fluorescence lifetimes calculated for the lipid-free penetratin peptides agree with the lifetimes and amplitude fractions reported by Clayton & Sawyer [36] for five variants of an amphipathic peptide, where the single Trp was moved along the sequence. Interaction of these peptides with lipid vesicles is accompanied by an increase of the α helix conformation, a disappearance of the short fluorescence lifetime, an increase of the two other lifetimes and of the mean average lifetime. In contrast, the amplitude of the long lifetime component is reduced to a few percent in penetratin, as are all lifetimes. Decrease of the mean Trp lifetimes in WT-, W48F- and W56F-penetratin variants measured in 100% TFE, was less than twofold compared to a fourfold to sevenfold decrease upon interaction with negatively charged lipid vesicles. The decrease of the mean Trp fluorescence lifetime of the 3Pro penetratin variant (RQPKIWFPNRRMPWKK) measured in 100% TFE was also around twofold (data not shown) although this peptide did not become α helical in TFE. This suggests that the conformational changes from random to α helical structure do not account for the observed Trp quenching. Other parameters, such as the interaction with PtdSer headgroups and/or the quenching of the Trp indole moiety by arginine and lysine side chains in penetratin peptides might account for this effect. Titrations of the WT-penetratin with PtdCho/PtdGro (80 : 20) and PtdCho/phosphatidic acid (80 : 20) vesicles induced only a blue shift of 10 nm but did not affect the fluorescence intensity (data not shown), suggesting a specific contribution of the PtdSer headgroup to fluorescence quenching. Peptide conformational changes accompanying binding of the penetratin peptide to negatively charged vesicles, might decrease the distance between one or more lysines or arginines and the Trp48 and 56 residues. Chen & Barkley [37] showed that the side chains of eight amino acids, including lysine, can quench Trp fluorescence. Similar quenching of Trp158 by Lys165 in the extracellular domain of human tissue factor was reported by Hasselbacher *et al.* [38]. Clark *et al.* further showed that Trp109 in the cellular retinoic acid-binding protein I is fluorescence-silent due to its interaction with the guanidino group of Arg111 [39].

WT and penetratin variants have a propensity to become α helical in 100% TFE, an α helix inducing solvent [40,41], and upon binding to negatively charged SUVs. Berlose *et al.* showed that WT-penetratin became α helical in 30% hexafluoroisopropanol, in perfluoro-*tert*-butanol and in the presence of SDS micelles [14]. Although the 3Pro variant had similar affinity to WT-penetratin for PtdCho/PtdSer (80 : 20, w/w) vesicles, it did not become α helical upon lipid association or when solubilized in TFE (data not shown). α Helix formation thus does not seem to be a prerequisite for lipid binding or for cell internalization, as shown by Derossi *et al.* [12].

In summary, our data suggest a mode of the penetratin peptide interaction with negatively charged PtdCho/PtdSer vesicles, where Trp48 is inserted more deeply into the lipid bilayer compared to Trp56. Peptide–lipid association is primarily due to electrostatic interactions between the positive charged Arg and Lys residues with the PtdSer headgroup, as suggested by fluorescence intensity and lifetime data. Penetratin translocation across the cell membrane is thus dependent upon its interaction with negatively charged lipids, which stabilizes the peptide α helical conformation.

REFERENCES

1. Gehring, W.J., Affolter, M. & Burglin, T. (1994) Homeodomain proteins. *Annu. Rev. Biochem.* **63**, 487–526.
2. Gehring, W.J., Qian, Y.Q., Billeter, M., Furukubo-Tokunaga, K., Schier, A.F., Resendez-Perez, D., Affolter, M., Otting, G. & Wuthrich, K. (1994) Homeodomain-DNA recognition. *Cell* **78**, 211–223.
3. Joliot, A.H., Triller, A., Volovitch, M., Pernelle, C. & Prochiantz, A. (1991) alpha-2,8-Polysialic acid is the neuronal surface receptor of antennapedia homeobox peptide. *New Biol.* **3**, 1121–1134.
4. Le Roux, I., Joliot, A.H., Bloch-Gallego, E., Prochiantz, A. & Volovitch, M. (1993) Neurotrophic activity of the antennapedia homeodomain depends on its specific DNA-binding properties. *Proc. Natl Acad. Sci. USA* **90**, 9120–9124.
5. Derossi, D., Joliot, A.H., Chassaing, G. & Prochiantz, A. (1994) The third helix of the antennapedia homeodomain translocates through biological membranes. *J. Biol. Chem.* **269**, 10444–10450.
6. Prochiantz, A. (1998) Peptide nucleic acid smugglers. *Nat. Biotechnol.* **16**, 819–820.
7. Derossi, D., Chassaing, G. & Prochiantz, A. (1998) Trojan peptides: the penetratin system for intracellular delivery. *Trends. Cell Biol.* **8**, 84–87.
8. Prochiantz, A. (1996) Getting hydrophilic compounds into cells: lessons from homeopeptides. *Curr. Opin. Neurobiol.* **6**, 629–634.
9. Theodore, L., Derossi, D., Chassaing, G., Llirbat, B., Kubes, M., Jordan, P., Chneiweiss, H., Godement, P. & Prochiantz, A. (1995) Intraneuronal delivery of protein kinase C pseudosubstrate leads to growth cone collapse. *J. Neurosci.* **15**, 7158–7167.
10. Troy, C.M., Derossi, D., Prochiantz, A., Greene, L.A. & Shelanski, M.L. (1996) Downregulation of Cu/Zn superoxide dismutase leads to cell death via the nitric oxide-peroxynitrite pathway. *J. Neurosci.* **16**, 253–261.
11. Pooga, M., Soomets, U., Hallbrink, M., Valkna, A., Saar, K., Rezaei, K., Kahl, U., Hao, J.X., Xu, X.J., Wiesenfeld-Hallin, Z., Hokfelt, T., Bartfai, T. & Langel, U. (1998) Cell penetrating PNA constructs regulate galanin receptor levels and modify pain transmission *in vivo*. *Nat. Biotechnol.* **16**, 857–861.
12. Derossi, D., Calvet, S., Trembleau, A., Brunissen, A., Chassaing, G. & Prochiantz, A. (1996) Cell internalization of the third helix of the antennapedia homeodomain is receptor-independent. *J. Biol. Chem.* **271**, 18188–18193.
13. de Kruijff, B., Cullis, P.R., Verkleij, A.J., Hope, M.J., van Echteld, C.J.A., Taraschi, T.F., van Hoogevest, P., Killian, J.A., Rietveld, A.G. & van der Steen, A.T.M. (1985) *Progress in Protein–Lipid Interactions.* pp. 89–142. Elsevier. Science Publishers, B.V., Amsterdam.
14. Berlose, J.P., Convert, O., Derossi, D., Brunissen, A. & Chassaing, G. (1996) Conformational and associative behaviours of the third helix of antennapedia homeodomain in membrane-mimetic environments. *Eur. J. Biochem.* **242**, 372–386.
15. de Kroon, A.I., Soekarjo, M.W., De Gier, J. & de Kruijff, B. (1990) The role of charge and hydrophobicity in peptide–lipid interaction: a comparative study based on tryptophan fluorescence

measurements combined with the use of aqueous and hydrophobic quenchers. *Biochemistry* **29**, 8229–8240.
16. Surewicz, W.K. & Epand, R.M. (1985) Role of peptide structure in lipid–peptide interactions: high-sensitivity differential scanning calorimetry and electron spin resonance studies of the structural properties of dimyristoylphosphatidylcholine membranes interacting with pentagastrin-related pentapeptides. *Biochemistry* **24**, 3135–3144.
17. Jain, M.K., Rogers, J., Simpson, L. & Gierasch, L.M. (1985) Effect of tryptophan derivatives on the phase properties of bilayers. *Biochim. Biophys. Acta* **816**, 153–162.
18. Bartlett, G.R. (1958) Phosphorus assay in column chromatography. *J.Biol. Chem.* **234**, 466–468.
19. Lakowicz, J.R., Laczko, G. & Gryczinski, I. (1985) 2-GHz frequency-domain fluorometer. *Rev. Sci. Instrum.* **57**, 2499–2506.
20. Vos, R., Engelborghs, Y., Izard, J. & Baty, D. (1995) Fluorescence study of the three tryptophan residues of the pore-forming domain of colicin A using multifrequency phase fluorometry. *Biochemistry* **34**, 1734–1743.
21. De Beuckeleer, K., Volckaert, G. & Engelborghs, Y. (1999) Time resolved fluorescence and phosphorescence properties of the individual tryptophan residues of barnase: evidence for protein–protein interactions. *Proteins* **36**, 42–53.
22. Eftink, M.R. & Ghiron, A. (1976) Exposure of tryptophanyl residues in proteins. Quantitative determination by fluorescence quenching studies. *Biochemistry* **15**, 672–680.
23. Lehrer, S.S. (1971) Solute perturbation of protein fluorescence. the quenching of the tryptophyl fluorescence of model compounds and of lysozyme by iodide ion. *Biochemistry* **10**, 3254–3263.
24. Bohm, G., Muhr, R. & Jaenicke, R. (1992) Quantitative analysis of protein far UV circular dichroism spectra by neural networks. *Protein Eng.* **5**, 191–195.
25. Chen, Y.H., Yang, J.T. & Martinez, H.M. (1972) Determination of the secondary structures of proteins by circular dichroism and optical rotatory dispersion. *Biochemistry* **11**, 4120–4131.
26. Eisenberg, D., Weiss, R.M. & Terwilliger, T.C. (1984) The hydrophobic moment detects periodicity in protein hydrophobicity. *Proc. Natl Acad. Sci. USA* **81**, 140–144.
27. Burstein, E.A., Vedenkina, N.S. & Ivkova, M.N. (1974) Fluorescence and the location of tryptophan residues in protein molecules. *Photochem. Photobiol.* **18**, 263–279.
28. Eftink, M.R. & Ghiron, C.A. (1977) Exposure of tryptophanyl residues and protein dynamics. *Biochemistry* **16**, 5546–5551.
29. Killian, J.A., Keller, R.C., Struyve, M., de Kroon, A.I., Tommassen, J. & de Kruijff, B. (1990) Tryptophan fluorescence study on the interaction of the signal peptide of the *Escherichia coli* outer membrane protein PhoE with model membranes. *Biochemistry* **29**, 8131–8137.
30. Drin, G., Mazel, M., Clair, P., Mathieu, D., Kaczorek, M. & Temsamani, J. (2001) Physico-chemical requirements for cellular uptake of pAntp peptide Role of lipid-binding affinity. *Eur. J. Biochem.* **268**, 1304–1314.
31. Joliot, A., Maizel, A., Rosenberg, D., Trembleau, A., Dupas, S., Volovitch, M. & Prochiantz, A. (1998) Identification of a signal sequence necessary for the unconventional secretion of Engrailed homeoprotein. *Curr. Biol.* **8**, 856–863.
32. Wieprecht, T., Dathe, M., Schumann, M., Krause, E., Beyermann, M. & Bienert, M. (1996) Conformational and functional study of magainin 2 in model membrane environments using the new approach of systematic double-D-amino acid replacement. *Biochemistry* **35**, 10844–10853.
33. Wieprecht, T., Beyermann, M. & Seelig, J. (1999) Binding of antibacterial magainin peptides to electrically neutral membranes: thermodynamics and structure. *Biochemistry* **38**, 10377–10387.
34. El Jastimi, R., Edwards, K. & Lafleur, M. (1999) Characterization of permeability and morphological perturbations induced by nisin on phosphatidylcholine membranes. *Biophys. J.* **77**, 842–852.
35. Udenfried, S. (1969) *Fluorescence Assay in Biology and Medicine.* Academic Press, New York.
36. Clayton, A.H. & Sawyer, W.H. (1999) Tryptophan rotamer distributions in amphipathic peptides at a lipid surface. *Biophys. J.* **76**, 3235–3242.
37. Chen, Y. & Barkley, M.D. (1998) Toward understanding tryptophan fluorescence in proteins. *Biochemistry* **37**, 9976–9982.
38. Hasselbacher, C.A., Rusinova, E., Waxman, E., Rusinova, R., Kohanski, R.A., Lam, W., Du Guha, A.J., Lin, T.C. & Polikarpov, I. (1995) Environments of the four tryptophans in the extracellular domain of human tissue factor: comparison of results from absorption and fluorescence difference spectra of tryptophan replacement mutants with the crystal structure of the wild-type protein. *Biophys. J.* **69**, 20–29.
39. Clark, P.L., Liu, Z.P., Zhang, J. & Gierasch, L.M. (1996) Intrinsic tryptophans of CRABPI as probes of structure and folding. *Protein Sci.* **5**, 1108–1117.
40. Bruch, M.D. & Gierasch, L.M. (1990) Comparison of helix stability in wild-type and mutant LamB signal sequences. *J. Biol. Chem.* **265**, 3851–3858.
41. Lehrman, S.R., Tuls, J.L. & Lund, M. (1990) Peptide alpha-helicity in aqueous trifluoroethanol: correlations with predicted alpha-helicity and the secondary structure of the corresponding regions of bovine growth hormone. *Biochemistry* **29**, 5590–5596.
42. Lindberg, M. & Gräslund, A. (2001) The position of the cell penetrating peptide penetratin in SDS micelles determined by NMR. *FEBS Lett.* **497**, 39–44.

P.M. Fischer
N.Z. Zhelev
S. Wang
J.E. Melville
R. Fåhraeus
D.P. Lane

Structure–activity relationship of truncated and substituted analogues of the intracellular delivery vector Penetratin

Authors' affiliations:
P.M. Fischer, N.Z. Zhelev, S. Wang, J.E. Melville, R. Fåhraeus and D.P. Lane, Cyclacel Limited, Dundee, UK.

Correspondence to:
Dr *Peter M. Fischer*
Cyclacel Limited
James Lindsay Place
Dundee
DD1 5JJ
UK
E-mail: pfischer@cyclacel.com

Dates:
Received 2 June 1999
Revised 2 August 1999
Accepted 26 August 1999

To cite this article:
Fischer, P.M., Zhelev, N.Z., Wang, S., Melville, J.E. Fåhraeus, R. & Lane, D.P. Structure-activity relationship of truncated and substituted analogues of the intracellular delivery vector Penetratin.
J. Peptide Res., 2000, 55, 163–172

Copyright Munksgaard International Publishers Ltd, 2000

ISSN 1397-002X

Key words: antennapedia homeoprotein; cell internalization; delivery vector; membrane translocation; Penetratin

Abstract: Peptides derived from the third α-helix of the homeodomain (residues 43–58; Penetratin) of Antennapedia, a *Drosophila* homeoprotein, were prepared by simultaneous multiple synthesis. Sets of N- and C-terminally truncated peptides, as well as a series of alanine substitution analogues, were studied. Cell penetration assays using human cell cultures with these peptides revealed that the C-terminal segment ^{52}Arg-Arg-Met-Lys-Trp-Lys-Lys^{58} of the parent sequence was necessary and sufficient for efficient cell membrane translocation. Individual Ala substitutions of the peptide's basic residues led to markedly decreased cell internalization ability, whereas replacement of hydrophobic residues was tolerated surprisingly well. Subcellular localization was seen to be affected by substitutions, with analogues being addressed preferentially to the cytosol or to the nucleus. Conformational constriction of the Penetratin sequence through placement and oxidation of flanking cysteine residues afforded a cyclic disulfide peptide which had lost most of its membrane translocation capacity.

Abbreviations: Amino acid and peptide nomenclature conforms to IUPAC-IUB rules (*Eur. J. Biochem.* 1984, **138**, 9–37). Ahx, 6-aminohexanoyl; APase, alkaline phosphatase. BSA, bovine serum albumin; DE MALDI-TOF MS, delayed-extraction matrix-assisted laser desorption ionization time-of-flight mass spectrometry; DIEA, diisoproplethylamine; DMF, dimethyl formamide; FCS, fetal calf serum; HOBt, 1-hydroxybenzotriazole; PBS, phosphate-buffered saline (10 mM phosphate, 150 mM NaCl, pH 7.4); PyBOP, benzotriazole-1-yl-oxy-tris-pyrrolidino-phosphonium hexafluorophosphate; RP-HPLC, reveresed-phase high-performance liquid chromatography; TFA, trifluoroacetic acid.

The clinical application of biomolecules such as oligonucleotides and polypeptides is generally hampered by poor cellular uptake. Because of their size and hydrophilic nature, most biomolecules do not readily translocate across the lipid bilayer of biological membranes. This problem can be overcome in experimental settings through various delivery techniques (microinjection, electroporation, association with cationic lipids, liposome encapsidation, etc.). However, routine use of biomolecules *in vivo* is generally precluded because of low transfer efficiency. Several polypeptides, including certain short peptides (1–3), have been proposed as carriers to achieve intracellular delivery of proteins and genes.

Homeoproteins are *trans*-activating factors involved in multiple morphological processes. They bind to DNA through a sequence of 60 amino acid residues, the so-called homeodomain. The structure of this domain consists of three α-helices, interrupted by a β-turn between helices 2 and 3 (4). The phylogenetic relationship between numerous homeoproteins is striking at the level of the homeodomain and particularly within the third α-helix. This helix is responsible for both the interaction with DNA by binding specifically to cognate sites in the genome (5), and the capacity of homeoproteins to translocated across cell membranes to cell nuclei in a nonspecific manner. It was shown that synthetic peptides, corresponding minimally to 16 residues of the third α-helix of the homeodomain from Antennapedia, a *Drosophila* homeoprotein, are capable of being internalized by cells (1). The peptide encompassing residues ^{43}Arg-Gln-Ile-Lys-Ile-Trp-Phe-Gln-Asn-Arg-Arg-Met-Lys-Trp-Lys-Lys^{58} of this protein is termed Penetratin. When covalently linked with 'molecular cargo', including polypeptides and oligonucleotides many times its own molecular mass (6, 7), this peptide apparently retains its membrane translocation properties and has therefore been proposed as a universal intracellular delivery vector (8). The mechanism by which Penetratin translocates across membranes remains largely unknown, although it is clear that no classical receptor is involved (9).

Here we present the results from a closer investigation of the structure–activity relationship of Penetratin, in terms of both the minimum active peptide length required and the relative importance of individual residues in the sequence. To this end we synthesized and assessed the cell penetration properties of C-terminally (peptides 1–10 in Table 1) and N-terminally (11–20) truncated derivatives of Penetratin, as well as a series of full-length peptides in which each residue in turn was substituted with alanine (21–36).

In order to probe the involvement of Penetratin's secondary structure during membrane translocation, we studied an analogue incorporating N- and C-terminal Cys residues in both linear reduced form (37) and in the conformationally restricted oxidized cyclic form (38).

37 Biotinyl-Ahx-Cys-Arg-Gln-Ile-Lys-Ile-Trp-Phe-Gln-Asn-Arg-Arg-Nle-Lys-Trp-Lys-Lys-Cys-OH

38 Biotinyl-Ahx-Cys-Arg-Gln-Ile-Lys-Ile-Trp-Phe-Gln-Asn-Arg-Arg-Nle-Lys-Trp-Lys-Lys-Cys-OH

In order to measure and visualize the subcellular distribution of Penetratin directly, we also prepared a Penetratin analogue (39) carrying a 5-carbonylfluoresceinyl label (b) rather than the biotinyl group (a) used for all other derivatives. This permitted us to inspect live cells after treatment with 39 using fluorescent microscopy.

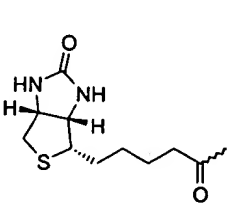

a

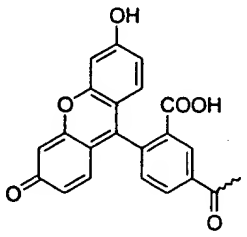

b

Experimental Procedures

General

The peptide deprotection/cleavage mixture used throughout was as follows: 0.75 : 0.5 : 0.5 : 0.25 : 10 (w/v/v/v/v) PhOH/H_2O/PhSMe/1,2-ethanedithiol/TFA (10). Analytical and preparative RP-HPLC was performed using Vydac 218TP54 (4.6 × 250 mm) and 218TP1022 (22 × 250 mm) columns, respectively. Flow rates of 1 mL/min for analytical runs and 9 mL/min for preparative work were used (at 25°C). Gradient elution with increasing amounts of MeCN in H_2O (containing 0.1% TFA) over 20 min (analalytical) and 40 min (preparative) was performed. Eluants were monitored at λ = 200–300 nm. Peptide samples were also analysed by DE MALDI-TOF mass spectrometry (Thermo-BioAnalysis Dynamo instrument). An α-cyano-4-hydroxycinnamic acid matrix (11) was used and the appropriate *m/z*

Table 1. **Antennapedia homeodomain peptide analogues synthesized and tested**

No.	Peptide
1	Biotinyl-βAla-Arg-Gln-Ile-Lys-Ile-Trp-Phe-Gln-Asn-Arg-Arg-Met-Lys-Trp-Lys-Lys-NH_2
2	Biotinyl-βAla-Arg-Gln-Ile-Lys-Ile-Trp-Phe-Gln-Asn-Arg-Arg-Met-Lys-Trp-Lys-NH_2
3	Biotinyl-βAla-Arg-Gln-Ile-Lys-Ile-Trp-Phe-Gln-Asn-Arg-Arg-Met-Lys-Trp-NH_2
4	Biotinyl-βAla-Arg-Gln-Ile-Lys-Ile-Trp-Phe-Gln-Asn-Arg-Arg-Met-Lys-NH_2
5	Biotinyl-βAla-Arg-Gln-Ile-Lys-Ile-Trp-Phe-Gln-Asn-Arg-Arg-Met-NH_2
6	Biotinyl-βAla-Arg-Gln-Ile-Lys-Ile-Trp-Phe-Gln-Asn-Arg-Arg-NH_2
7	Biotinyl-βAla-Arg-Gln-Ile-Lys-Ile-Trp-Phe-Gln-Asn-Arg-NH_2
8	Biotinyl-βAla-Arg-Gln-Ile-Lys-Ile-Trp-Phe-Gln-Asn-NH_2
9	Biotinyl-βAla-Arg-Gln-Ile-Lys-Ile-Trp-Phe-Gln-NH_2
10	Biotinyl-βAla-Arg-Gln-Ile-Lys-Ile-Trp-NH_2
11	Biotinyl-βAla-Gln-Ile-Lys-Ile-Trp-Phe-Gln-Asn-Arg-Arg-Met-Lys-Trp-Lys-Lys-NH_2
12	Biotinyl-βAla-Ile-Lys-Ile-Trp-Phe-Gln-Asn-Arg-Arg-Met-Lys-Trp-Lys-Lys-NH_2
13	Biotinyl-βAla-Lys-Ile-Trp-Phe-Gln-Asn-Arg-Arg-Met-Lys-Trp-Lys-Lys-NH_2
14	Biotinyl-βAla-Ile-Trp-Phe-Gln-Asn-Arg-Arg-Met-Lys-Trp-Lys-Lys-NH_2
15	Biotinyl-βAla-Trp-Phe-Gln-Asn-Arg-Arg-Met-Lys-Trp-Lys-Lys-NH_2
16	Biotinyl-βAla-Phe-Gln-Asn-Arg-Arg-Met-Lys-Trp-Lys-Lys-NH_2
17	Biotinyl-βAla-Gln-Asn-Arg-Arg-Met-Lys-Trp-Lys-Lys-NH_2
18	Biotinyl-βAla-Asn-Arg-Arg-Met-Lys-Trp-Lys-Lys-NH_2
19	Biotinyl-βAla-Arg-Arg-Met-Lys-Trp-Lys-Lys-NH_2
20	Biotinyl-βAla-Arg-Met-Lys-Trp-Lys-Lys-NH_2
21	Biotinyl-βAla-Ala-Gln-Ile-Lys-Ile-Trp-Phe-Gln-Asn-Arg-Arg-Met-Lys-Trp-Lys-Lys-NH_2
22	Biotinyl-βAla-Arg-Ala-Ile-Lys-Ile-Trp-Phe-Gln-Asn-Arg-Arg-Met-Lys-Trp-Lys-Lys-NH_2
23	Biotinyl-βAla-Arg-Gln-Ala-Lys-Ile-Trp-Phe-Gln-Asn-Arg-Arg-Met-Lys-Trp-Lys-Lys-NH_2
24	Biotinyl-βAla-Arg-Gln-Ile-Ala-Ile-Trp-Phe-Gln-Asn-Arg-Arg-Met-Lys-Trp-Lys-Lys-NH_2
25	Biotinyl-βAla-Arg-Gln-Ile-Lys-Ala-Trp-Phe-Gln-Asn-Arg-Arg-Met-Lys-Trp-Lys-Lys-NH_2
26	Biotinyl-βAla-Arg-Gln-Ile-Lys-Ile-Ala-Phe-Gln-Asn-Arg-Arg-Met-Lys-Trp-Lys-Lys-NH_2
27	Biotinyl-βAla-Arg-Gln-Ile-Lys-Ile-Trp-Ala-Gln-Asn-Arg-Arg-Met-Lys-Trp-Lys-Lys-NH_2
28	Biotinyl-βAla-Arg-Gln-Ile-Lys-Ile-Trp-Phe-Ala-Asn-Arg-Arg-Met-Lys-Trp-Lys-Lys-NH_2
29	Biotinyl-βAla-Arg-Gln-Ile-Lys-Ile-Trp-Phe-Gln-Ala-Arg-Arg-Met-Lys-Trp-Lys-Lys-NH_2
30	Biotinyl-βAla-Arg-Gln-Ile-Lys-Ile-Trp-Phe-Gln-Asn-Ala-Arg-Met-Lys-Trp-Lys-Lys-NH_2
31	Biotinyl-βAla-Arg-Gln-Ile-Lys-Ile-Trp-Phe-Gln-Asn-Arg-Ala-Met-Lys-Trp-Lys-Lys-NH_2
32	Biotinyl-βAla-Arg-Gln-Ile-Lys-Ile-Trp-Phe-Gln-Asn-Arg-Arg-Ala-Lys-Trp-Lys-Lys-NH_2
33	Biotinyl-βAla-Arg-Gln-Ile-Lys-Ile-Trp-Phe-Gln-Asn-Arg-Arg-Met-Ala-Trp-Lys-Lys-NH_2
34	Biotinyl-βAla-Arg-Gln-Ile-Lys-Ile-Trp-Phe-Gln-Asn-Arg-Arg-Met-Lys-Ala-Lys-Lys-NH_2
35	Biotinyl-βAla-Arg-Gln-Ile-Lys-Ile-Trp-Phe-Gln-Asn-Arg-Arg-Met-Lys-Trp-Ala-Lys-NH_2
36	Biotinyl-βAla-Arg-Gln-Ile-Lys-Ile-Trp-Phe-Gln-Asn-Arg-Arg-Met-Lys-Trp-Lys-Ala-NH_2

range was calibrated using authentic peptide standards in the *m/z* range 1000–2600.

Simultaneous multiple synthesis of peptides 1–36

Peptides were synthesized using a Multipin Peptide Synthesis Kit (Chiron Technologies Pty. Ltd, Clayton, VIC, Australia). Peptide chains were assembled on 'Macro Crowns' (SynPhase HM Series I, Rink Amide Linker; 5.3 μmol/crown) using Fmoc-amino acids (100 mM in DMF) and PyBOP/HOBt/DIEA (1 : 1 : 1.5) coupling chemistry. The amino acid side-chain-protecting groups were 2,2,5,7,8-pentamethylchroman-6-sulfonyl (Arg), trityl (Asn and Gln) and *t*-butyloxycarbonyl (Lys and Trp). Activated amino acid solutions were dispensed using a PinAID device (Chiron Technologies). Coupling reactions were allowed to proceed for a minimum of 4 h. All other chain assembly manipulations, including repetitive deprotection reactions

(20% piperidine in DMF) and washing cycles (DMF and MeOH), were carried out according to procedures set out in the kit manual. After coupling and deprotection of the N-terminal βAla residues (+)-biotin (300 mM in DMF) was coupled (chemistry as above for amino acids) for 4 h. After washing and drying, the 'Macro Crowns' were removed from the synthesis device and placed into 10 mL capped polypropylene tubes. To each tube was added 1.5 mL of cleavage/deprotection mixture. After 2 h, the 'Macro Crowns' were removed and washed with 0.5 mL each of neat TFA. To each tube containing the combined cleavage mixtures and washings Et_2O (8 mL) was added. After cooling to 4°C, the precipitated peptides were collected by centrifugation (4 min at 1950×g) and decantation. The pellets were resuspended in Et_2O (5 mL/tube). The suspensions were again cooled and the peptides were isolated as before. The washing process was repeated once more before the crude peptides were dried *in vacuo*.

The crude peptides were redissolved in 0.1% aq. TFA using sonication (2 mL/sample) and were applied to primed (MeOH then 0.1% aq. TFA) solid-phase extraction cartridges (Merck LiChrolut RP-18, 500 mg). These were successively washed (2 × 2 mL 0.1% aq. TFA each) and eluted (2 mL 0.1% TFA in 6 : 4 MeCN/H_2O). The eluates were evaporated to dryness by vacuum centrifugation. Yields and analytical data for the title compounds are summarized in Table 2.

Reduced linear and oxidized cyclic peptides 37 and 38

The peptide sequence was assembled on Fmoc-Cys(Trt)-resin (*p*-hydroxymethylphenoxyacetic acid handle, 0.50 mmol/g functionality, 0.50 g, 0.25 mmol; ABI 401418) using an ABI 433A Peptide Synthesizer (Perkin-Elmer Applied Biosystems) and standard '0.25 mmol FastMoc MonPrevPk' chemistry. After final Fmoc-deprotection and washing (Et_2O), the peptidyl resin was dried *in vacuo* (1.43 g, 91%). An aliquot (285 mg, ≈ 0.05 mmol) of this material was resuspended in DMF, drained and reacted with biotinamidocaproate *N*-hydroxysuccinimide ester (137 mg, 0.3 mmol), HOBt (50 mg, 0.3 mmol) and DIEA (0.14 mL 0.8 mmol) in DMF (3 mL) for 18 h under N_2. The resin was then washed successively with DMF, CH_2Cl_2 and Et_2O, before being dried *in vacuo*.

The above biotinylated peptidyl resin (290 mg, ≈ 0.05 mmol) was treated with cleavage/deprotection mixture (5 mL) for 2.5 h. Resin residue was then filtered off. The filtrate was treated with Et_2O (45 mL), the mixture was cooled and the precipitated peptide was collected by centrifugation (2 min at 1250×g). The crude biotinylated peptide (141 mg, *ca.* quant.) was washed twice more with Et_2O in a similar manner to before being dried *in vacuo*. A sample (20 mg) of this material was dissolved in 0.1% aq. TFA (2 mL), the solution was filtered and fractionated by preparative RP-HPLC. Fractions containing pure material (by analytical RP-HPLC) were pooled and lyophilized to afford pure peptide 37 (12.1 mg). Analytical RP-HPLC: t_R = 20.8 min, purity > 99% at λ = 214 nm (20–30% MeCN gradient). DE MALDI-TOF MS: $[MH]^+$ = 2776, $[MH]^{2+}$ = 1389 ($C_{127}H_{205}N_{39}O_{25}S_3$ = 2774.43).

Crude peptide 37 (before preparative RP-HPLC, 35 mg) was dissolved in aq. NH_4HCO_3 solution (0.1 M, 70 mL). The uncapped mixture was stirred for 18 h at room temperature. The resulting suspension was then acidified to pH 4 with AcOH (≈ 2 mL) to yield a clear solution, which was evaporated to dryness by vacuum centrifugation for 18 h. The residue was redissolved in 0.1% aq. TFA (2 mL) and purified by preparative RP-HPLC in a similar manner to the above reduced precursor 37 except that the gradient was developed from 20 to 30% MeCN. After lyophilization, pure peptide 38 (4.5 mg) was obtained. Analytical RP-HPLC: t_R = 15.7 min, purity > 99% at λ = 214 nm (20–30% gradient). DE MALDI-TOF MS: $[MH]^+$ = 2774, $[MH]^{2+}$ = 1388 ($C_{127}H_{203}N_{39}O_{25}S_3$ = 2772.42).

Fluorescein-labelled Penetratin 39

The sequence was assembled in a similar fashion as described for peptide 37, except that Fmoc-Lys (Boc)-Resin (0.5 mmol/g loading; ABI 401425) was used. The H-βAla-Arg(Pmc)-Gln(Trt)-Ile-Lys(Boc)-Ile-Trp-Phe-Gln(Trt)-Asn (Trt)-Arg(Pmc)-Arg(Pmc)-Met-Lys(Boc)-Trp-Lys(Boc)-Lys (Boc)-Resin (300 mg, ≈ 0.055 mmol) was reacted with 5-carboxyfluorescein (103 mg, 0.27 mmol; Sigma C 0537), PyBOP (142 mg, 0.27 mmol), HOBt (37 mg, 0.27 mmol) and DIEA (71 μL, 0.41 μmol) in DMF (5 μL) under N_2 and in the dark for 18 h. It was then washed (DMF, CH_2Cl_2 and Et_2O) and dried *in vacuo*. After treatment for 2 h with the cleavage/deprotection mixture (12 mL) in the dark and work-up as above, crude peptide was obtained (183 mg). An aliquot (90 mg) was purified by preparative RP-HPLC to afford pure peptide after lyophilization (38 mg). Analytical RP-HPLC: t_R = 15.7 min, purity > 99% at λ = 214 nm (22.5–32.5% gradient). DE MALDI-TOF MS: $[MH]^+$ = 2677, [2 MH] = 5359 ($C_{128}H_{183}N_{35}O_{27}S$ = 2676.11).

Table 2. **Chromatographic and mass spectrometric analysis of peptides 1–36**

No.	Formula	M_r	MS[a] [MH]$^+$	mg[b]	Yield µmol	%[c]	Analytical t_R (min)[d]	RP-HPLC Purity (%)[e]
1	$C_{117}H_{188}N_{38}O_{22}S_2$	2543.12	2544.1	6.7	2.6	50	19.0	78
2	$C_{111}H_{176}N_{36}O_{21}S_2$	2414.95	2416.0	6.8	2.8	53	19.4	78
3	$C_{105}H_{164}N_{34}O_{20}S_2$	2286.77	2287.8	4.8	2.1	40	20.3	79
4	$C_{96}H_{154}N_{32}O_{19}S_2$	2100.56	2101.6	7.5	3.6	67	18.5	75
5	$C_{86}H_{142}N_{30}O_{16}S_2$	1972.39	1973.4	6.5	3.3	62	19.1	81
6	$C_{93}H_{133}N_{29}O_{17}S$	1841.20	1842.2	5.6	3.1	58	18.5	98
7	$C_{77}H_{121}N_{25}O_{16}S$	1685.01	1686.0	7.0	4.2	78	19.0	95
8	$C_{71}H_{109}N_{21}O_{15}S$	1528.82	1529.8	4.8	3.1	59	19.7	95
9	$C_{67}H_{103}N_{19}O_{13}S$	1414.72	1415.7	4.8	3.4	64	20.2	90
10	$C_{53}H_{86}N_{16}O_{10}S$	1139.42	1140.4	3.2	2.8	53	17.9	93
11	$C_{111}H_{176}N_{34}O_{21}S_2$	2386.93	2387.9	5.1	2.1	40	19.5	82
12	$C_{106}H_{168}N_{32}O_{19}S_2$	2258.80	2259.8	5.0	2.2	42	19.8	85
13	$C_{100}H_{157}N_{31}O_{18}S_2$	2145.65	2146.7	5.8	2.7	51	17.6	90
14	$C_{94}H_{145}N_{29}O_{17}S_2$	2017.47	2018.5	6.6	3.3	62	19.1	87
15	$C_{88}H_{134}N_{28}O_{16}S_2$	1904.32	1905.3	5.3	2.8	53	17.9	90
16	$C_{77}H_{124}N_{26}O_{15}S_2$	1718.11	1719.1	5.3	3.1	58	14.9	91
17	$C_{68}H_{115}N_{25}O_{14}S_2$	1570.93	1571.9	5.6	3.6	67	12.2	93
18	$C_{63}H_{107}N_{23}O_{12}S_2$	1442.80	1443.8	4.4	3.0	57	12.4	93
19	$C_{59}H_{101}N_{21}O_{10}S_2$	1328.70	1329.7	5.1	3.9	73	12.7	94
20	$C_{52}H_{85}N_{17}O_9S_2$	1172.51	1173.5	5.0	4.3	81	13.2	96
21	$C_{114}H_{181}N_{35}O_{11}S_2$	2458.01	2459.0	5.7	2.3	44	16.8	66
22	$C_{115}H_{185}N_{37}O_{21}S_2$	2486.00	2487.1	6.2	2.5	47	16.9	79
23	$C_{114}H_{182}N_{38}O_{22}S_2$	2501.04	2502.0	5.8	2.3	44	12.9	80
24	$C_{114}H_{181}N_{37}O_{22}S_2$	2486.00	2487.0	6.4	2.6	48	17.6	76
25	$C_{114}H_{182}N_{38}O_{22}S_2$	2501.04	2502.0	6.8	2.7	51	15.7	80
26	$C_{109}H_{183}N_{37}O_{22}S_2$	2427.99	2429.0	6.7	2.7	52	12.5	80
27	$C_{111}H_{184}N_{38}O_{22}S_2$	2467.02	2468.0	6.1	2.5	47	12.8	78
28	$C_{115}H_{185}N_{37}O_{21}S_2$	2486.07	2487.1	6.5	2.6	49	15.9	79
29	$C_{116}H_{187}N_{37}O_{21}S_2$	2500.09	2501.1	5.7	2.3	43	16.2	75
30	$C_{114}H_{181}N_{35}O_{22}S_2$	2458.01	2459.0	5.6	2.3	43	18.7	77
31	$C_{114}H_{181}N_{35}O_{22}S_2$	2458.01	2459.0	7.5	3.1	58	16.8	77
32	$C_{115}H_{184}N_{38}O_{22}S_2$	2483.00	2484.0	6.4	2.6	49	15.4	96
33	$C_{114}H_{181}N_{37}O_{22}S_2$	2486.03	2487.0	6.8	2.7	52	16.6	79
34	$C_{109}H_{183}N_{37}O_{22}S_2$	2427.99	2429.0	8.5	3.5	66	14.3	83
35	$C_{114}H_{181}N_{37}O_{22}S_2$	2486.03	2487.0	9.0	3.6	68	16.5	78
36	$C_{114}H_{181}N_{37}O_{22}S_2$	2486.03	2487.0	10.1	4.0	76	16.4	73

a. By DE MALDI-TOF MS. b. After solid-phase extraction and vacuum centrifugation. c. Relative to 5.3 µmol loading of synthesis 'crowns'. d. Gradient 5–35% (peptides 1–20) and 15–35% acetonitrile (peptides 21–36) in 0.1% aq. TFA over 20 min. e. From chromatogram integration (λ = 214 nm).

Peptide internalization assay

HaCaT cells (immortalized 'normal' human fibroblast cell line) or A549 (human lung cancer cell line) were seeded into 96-well plates at 50 000 cells per well in Dulbecco's modified Eagle's medium (DMEM) with 10% FCS and antibiotics. After overnight incubation, peptides were prepared as dilution series in cell medium and were added to the cells. At the end of the incubation period (usually 10 and 60 min at 37 or 4°C), the cells were rinsed three times with PBS and fixed for 20 min at –20°C in EtOH/AcOH (95 : 5). After fixation, the cells were made permeable by

treatment for 10 min with PBS containing 3% Tween-20. Endogenous APase activity was neutralized by incubation at 65°C for 60 min and the wells were then blocked with 1% BSA in PBS. Cells were incubated for 30 min at room temperature with APase-streptavidin (Pierce Chemical Co., Rockford, IL, USA) in 0.1% BSA in PBS and washed extensively with PBS. Freshly prepared substrate solution [1 mg/mL *p*-nitrophenyl phosphate disodium (Pierce Chemical Co.) in 10 mM diethanolamine (pH 9.5) containing 0.5 mM $MgCl_2$] was added to each well and incubated until sufficient colour had developed (≈ 30 min). The enzymatic reaction was stopped by adding 50 µL 2 M aq. NaOH to each well. APase activity was measured spectrophotometrically at 405 nm.

Internalization assays for fluorescent peptides were performed in a similar way. After the incubation period the cells were rinsed extensively with PBS, until no fluorescence was detected in the washings, and the fluorescence intensity measured using a Biolite F1 fluorescence plate reader (BIO-TEK Instruments, Inc.).

Visualization of peptide internalization

HaCaT or A549 cells were seeded into eight-well chamber slides at 50 000 cells per well in DMEM with 10% FCS and antibiotics. After peptide treatment, fixation and permeabilization as above, the slides were incubated with streptavidin–FITC (Pierce Chemical Co.) in PBS for 30 min at room temperature, washed extensively with PBS and mounted in Hydromount (Merck-BDH, Poole, UK). To visualize the internalization of fluorescent peptides on live (unfixed) cells, fluorescent peptides were prepared in cell medium at 5 µM and added to cells for 30 min. At the end of the incubation period the cells were rinsed three times with PBS and the distribution of the fluorescence was analysed immediately on a Nikon Eclipse E800 fluorescence microscope. Images were captured with a Kodak DCS 420 digital camera and analysed using Adobe 5.0 software.

Results and Discussion

Peptide synthesis

Peptides 1–36 were prepared simultaneously using the so-called Multipin® method (12). On average two coupling/deprotection cycles were performed per day and the entire synthesis, including biotinylation, cleavage/deprotection, purification by solid-phase extraction and analysis, was completed within a fortnight. The isolated and purified yields of the peptides ranged from 40 to 81% and purities were 66–98% (Table 2). The excellent quality of the peptides is demonstrated in Fig. 1. The main impurities observed (MS, data not shown) were Met(O)-containing peptides (leading peaks on traces in Fig. 1). All sequences not containing Met (6–10 and 32) were obtained in > 90% purity. Methionine sulfoxide formation appears to be a general problem attendant in the Multipin method, presumably due to oxidation during the extended air-drying cycles after the acylation and deprotection steps. In principle it is possible to back-reduce Met(O) in peptides; e.g. on an analytical scale we were able to convert the Met(O)-containing impurity to 1 cleanly using NH_4I/Me_2S in TFA (13) (results not shown).

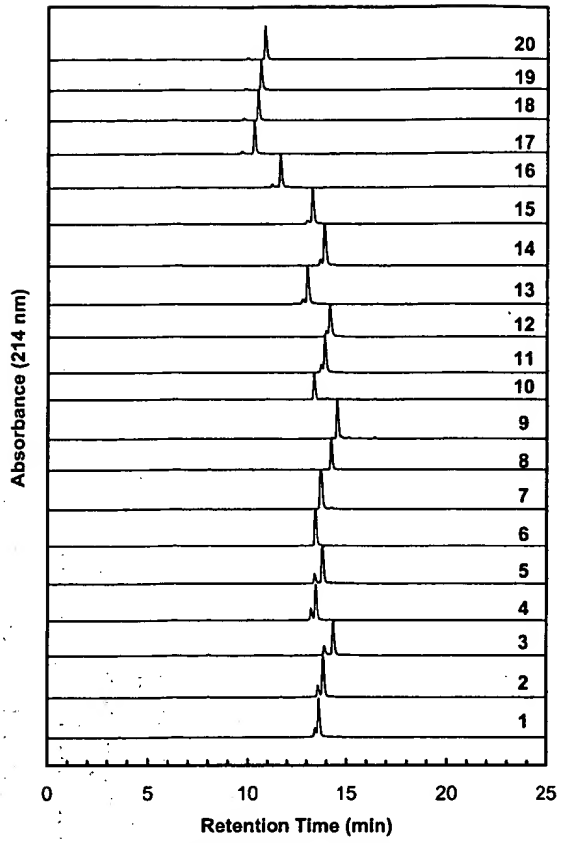

Figure 1. RP-HPLC analysis of simultaneously synthesized peptides. After purification by solid-phase extraction, the peptides were redissolved at ≈ 1 mg/mL in 0.1% aq. TFA and 15 µL of each solution was injection onto an analytical column (Vydac 218TP54, 1 mL/min, 0–60% MeCN in 0.1% aq. TFA over 20 min).

The linear biotinylated Penetratin analogue containing N- and C-terminal Cys residues could be cyclized cleanly to the disulfide peptide by air oxidation at elevated pH and using a peptide concentration of 0.5 mg/mL.

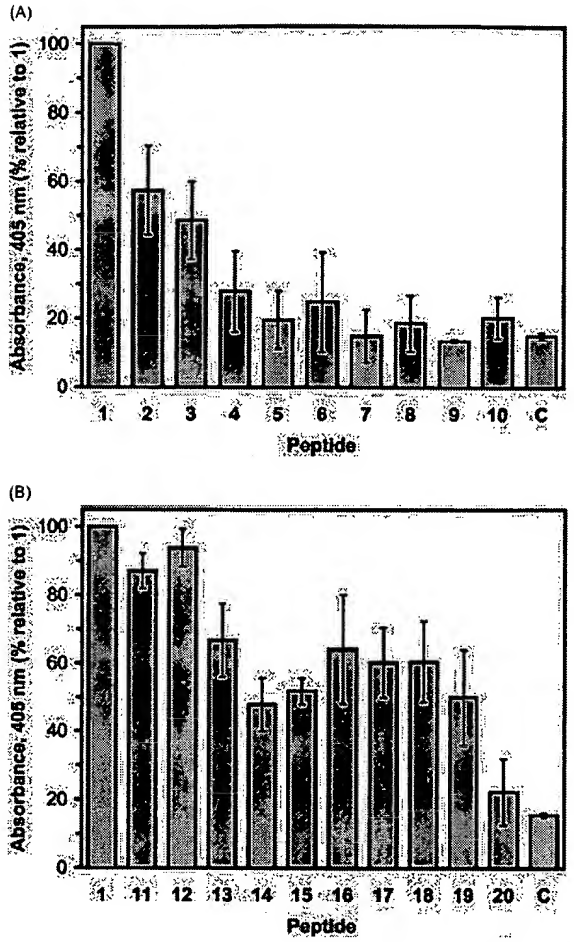

Figure 2. Cell internalization of truncated Penetratin analogues. Cells were treated for 60 min with C-terminally (2–10) or N-terminally (11–20) truncated biotinylated Penetratin analogues at a concentration of 40 μM. C refers to an unrelated biotinylated peptide control. Cellular uptake was quantitated as described in Experimental procedures. The averages of three independent experiments (± 1 SD) are shown.

Determination of minimal active sequence

The 16-mer peptide subtending residues 43–58 of the Antennapedia homeodomain was originally identified as the minimal sequence retaining efficient translocation properties using peptides corresponding to residues 41–60, 43–58, 41–55 and 46–60. Of these, only the former two were found to internalize into neuronal cells (1). Our results (Fig. 2) confirm that truncation of even a single residue from the C-terminus of the 16-mer (43–58) peptide (1) resulted in considerable loss of membrane translocation properties (peptide 2). Further stepwise truncation rapidly resulted in peptides that were almost inactive. Successive truncation from the N-terminus of peptide 1, however, presented a different picture. Little activity was lost upon the first three truncations (11–13) but only about half of the original signal was left with derivatives 14 and 15. However, at the 10-mer to 7-mer (16–19) stage, membrane translocation efficiency increased, reaching ≈ 60% relative to control peptide 1, before a severe decrease was observed with the C-terminal 6-mer peptide 20. We found this interesting pattern to be reproducible in several independent experiments. While values for only one peptide concentration are shown in Fig. 2, we established dose–response curves for each individual peptide and found that the same pattern was seen, regardless of peptide concentration. Furthermore, we examined all the peptides for nonspecific binding in the absence of cells and found this to be uniform and negligible (results not shown). Moreover, the internalization assay data were in agreement with fluorescence intensity measurements made after visualization of peptide internalization.

Effect of residue substitutions

Next we asked which of the residues in the 16-mer peptide 1 were of particular importance for the interesting biological activity seen. The results using a set of peptides in which each residue in turn had been substituted with Ala (peptides 21–36) are shown in Fig. 3. Overall, the most dramatic changes occurred upon modification within the segment encompassing the seven C-terminal residues, consistent with the findings using the truncated peptides (see above). All five C-terminal basic residues (peptides 30, 31, 33, 35 and 36) were particularly sensitive to substitution. Of the remaining two basic residues (peptides 21 and 24) only Lys^4 was poorly substituted by Ala. Surprisingly, all the hydrophobic residues, including Asn and Gln, were not particularly sensitive to Ala substitution, with the exception of Gln^2 (peptide 22) and Trp^{14} (peptide 34). It can be expected that, to some extent, this picture is due to the fact that Ala substitution for these residues is more conservative than for the basic amino acids. Nevertheless, the results clearly show that there are no very stringent requirements for any particular hydrophobic residue. It has been shown elsewhere that, for example, both Ile residues can be substituted with Val, apparently without loss of activity (14). Furthermore, Met^{12} is freely exchangeable with either Leu or Nle (results not shown). A double mutant peptide containing Phe in place of both Trp residues was reported to internalize poorly (1).

Importance of peptide conformation

Studies using analogues in which one (Gln^8) or three (Gln^8, Ile^3 and Lys^{13}) residues had been substituted with Pro

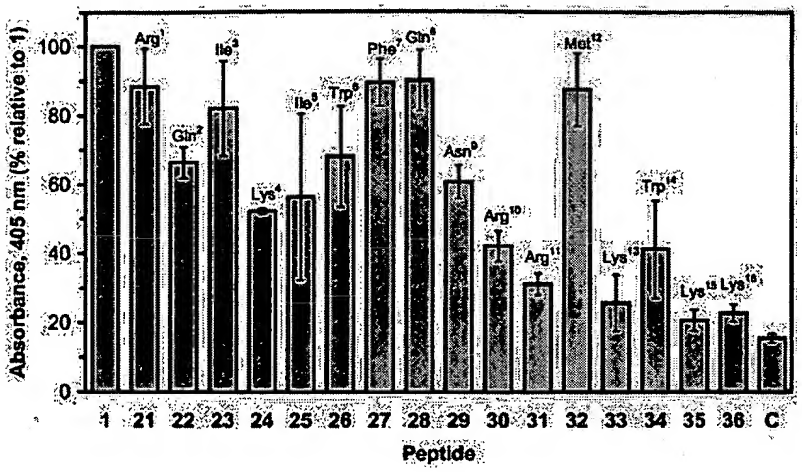

Figure 3. Alanine scan of Penetratin. Cells were treated with the Ala substitution peptide analogues 21–36. Assay procedures were identical to those described in Fig. 2.

showed that even the triple mutant was still able to translocate across cell membranes to some extent (9). Furthermore, analysis of the former Pro-containing peptide in a membrane-mimetic environment suggested that while the native peptide may favour an amphipathic helical conformation, this is not mandatory for efficient membrane translocation (15). Finally, Antennapedia homeoprotein 43–58 peptides with inverted or retro-inverted sequences apparently retain membrane translocation properties, presumably due to the fact that they can still form the necessary amphipathicity pattern, whatever this may be, necessary for biological function (9, 14).

We attempted to shed further light on this question by constraining the peptide's conformation through cyclization. Figure 4 shows that both peptides 1 and a linear Cys-analogue 37 are well internalized, while the cyclic peptide 38 shows almost no cell internalization ability (the apparent lower activity of 37 with respect to 1 may be due to relatively facile oxidation under physiological conditions).

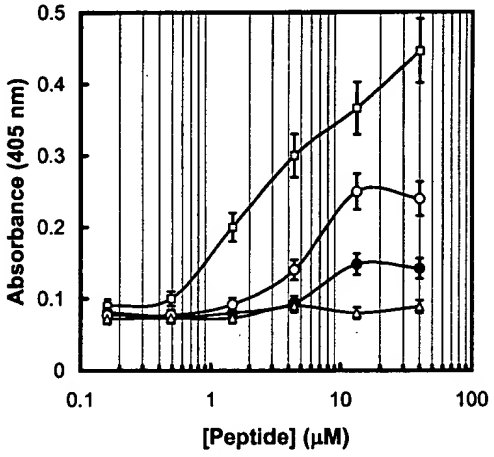

Figure 4. Effect of cyclization upon cell internalization capacity of Penetratin. Cells were treated for 60 min with biotinylated peptides (positive control 1, □; linear Cys-peptide 37, ○; cyclic Cys peptide 38, ●; control peptide with unrelated sequence, △). The assay procedures were identical to those described in Fig. 2.

Subcellular localization

Although the use of biotinylated peptides in cell internalization studies is convenient, it necessitates cell rupture and fixation after peptide internalization in order to achieve access of the labelled avidin marker to the biotin groups. Because we were particularly interested in the subcellular localization of our Penetratin variants, we prepared

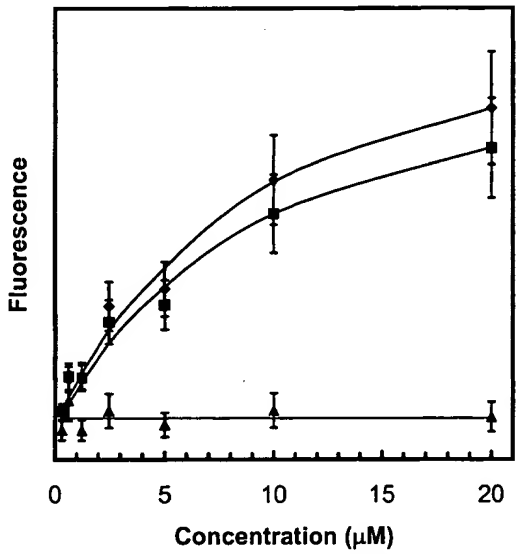

Figure 5. Direct measurement of peptide internalization into live cells. Cells were treated with the fluorescent peptide 39 for 10 min (■) and 60 min (◆) or with a control peptide (fluorescein-labelled peptide with unrelated sequence). They were then rinsed with PBS until no fluorescence was detected in the washings and read immediately in a fluorimeter.

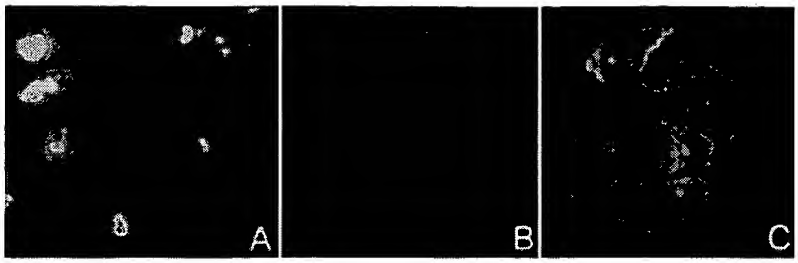

Figure 6. Visualization of Penetratin cell internalization by fluorescence miroscopy. (A) Peptide **1**, and (B) unrelated biotinylated peptide, show the intracellular distribution after cell fixation and treatment with FITC-avidin. (C) The distribution of fluorescent peptide **39** in unfixed cells. Peptide incubation was for 30 min at a concentration of 5 μM throughout.

fluorescein-labelled Penetratin (**39**), which allowed us to study and measure (Fig. 5) cell internalization without the possibility of observing artefacts emanating from the cell manipulations necessary with the biotinylated peptides. As can be seen in Fig. 6, biotinylated Penetratin **1** localizes predominantly to the cell nucleus and accumulates in the nucleoli, with a lower concentration in the cytosol. Clearly the distribution is very similar when the direct fluorescent probe **39** is used, thus validating the indirect biotin–avidin visualization approach. The fact that Penetratin appears to localize mainly to the nucleus shows that this peptide can in fact translocate across both plasma and nuclear membranes. Owing to the small size and basic nature of the peptides, import into the nucleus may be simply due to free diffusion through the pores present in nuclear membranes. Nuceolar accumulation may be due to nonspecific binding of the positively charged peptide to DNA.

It has been noted for a number of Antennapedia homeodomain peptides that membrane translocation is energy-independent and it therefore seems likely that cell internalization through classical receptor-mediated endocytosis is not involved (9). In order to ascertain that our compounds behave similarly, we compared quantitatively cell internalization at 4 and 37°C for a number of the peptides reported here, including the minimized peptide **19**. In all cases we measured membrane translocation efficiencies that were not significantly different at the two temperatures.

Conclusion

We are currently further extending our knowledge about the structure–activity relationships of Penetratin, including the use of multiple residue substitution analogues. Furthermore, we are studying the utility of the shortened Penetratin analogues **11–19** as cell internalization vectors for molecular cargoes, including peptides, proteins, oligonucleotides and other potentially useful molecules exhibiting poor cellular uptake.

Acknowledgements: We thank Ms Susan Duff and Mr Kevin Stewart for technical assistance in tissue culture and penetration assay work. We are grateful to Professor Alain Prochiantz for helpful discussions.

References

1. Derossi, D., Joliot, A.H., Chassaing, G. & Prochiantz, A. (1994) The third helix of the Antennapedia homeodomain translocates through biological membranes. *J. Biol. Chem.* **269**, 10444–10450.
2. Vivès, E., Brodin, P. & Lebleu, B. (1997) A truncated HIV-1 Tat protein basic domain rapidly translocates through the plasma membrane and accumulates in the cell nucleus. *J. Biol. Chem.* **272**, 16010–16017.
3. Pooga, M., Hällbrink, M., Zorko, M. & Langel, Ü. (1998) Cell penetration by transportan. *FASEB J.* **12**, 67–77.
4. Gehring, W.J., Müller, M., Affolter, M., Percival-Smith, A., Billeter, M., Qian, Y.Q., Otting, G. & Wüthrich, K. (1990) The structure of the homeodomain and its functional implications. *Trends Genet.* **6**, 323–329.
5. Le Roux, I., Joliot, A.H., Bloch-Gallego, E., Prochiantz, A. & Volovitch, M. (1993) Neurotrophic activity of the Antennapedia homeodomain depends on its specific DNA-binding properties. *Proc. Natl Acad. Sci. USA* **90**, 9120–9124.
6. Kato, D., Miyazawa, K., Ruas, M., Starborg, M., Wada, I., Oka, T., Sakai, T., Peters, G. & Hara, E. (1998) Features of replicative senescence induced by direct addition of Antennapedia-p16INK4A fusion protein human diploid fibroblasts. *FEBS Lett.* **427**, 203–208.
7. Pooga, M., Soomets, U., Hällbrink, M., Valkna, A., Saar, K., Rezaei, K., Kahl, U., Hao, J.-X., Xu, X.-J., Wiesenfeld-Hallin, Z., Hokfelt, T., Bartfai, T. & Langel Ü. (1998) Cell penetrating PNA constructs regulate galanin receptor levels and modify pain transmission *in vivo*. *Nature Biotechnol.* **16**, 857–861.
8. Derossi, D., Chassaing, G. & Prochiantz, A. (1998) Trojan peptides: the Penetratin system for intracellular delivery. *Trends Cell Biol.* **8**, 84–87.

9. Derossi, D., Calvet, S., Trembleau, A., Brunissen, A., Chassaing, G. & Prochiantz, A. (1996) Cell internalization of the third helix of the Antennapedia homeodomain is receptor-independent. *J. Biol. Chem.* **271**, 18188–18193.
10. King, D.S., Fields, C.G. & Fields, G.B. (1990) A cleavage method which minimizes side reactions following Fmoc solid phase peptide synthesis. *Int. J. Peptide Protein Res.* **36**, 255–266.
11. Beavis, R.C., Chaudhary, T. & Chait, B.T. (1992) α-Cyano-4-hydroxycinnamic acid as a matrix for matrix-assisted laser desorption mass spectrometry. *Org. Mass Spectrometry* **27**, 156–158.
12. Valerio, R.M., Bray, A.M., Campbell, R.A., Dipasquale, A., Margellis, C., Rodda, S.J., Geysen, H.M. & Maeji, N.J. (1993) Multipin peptide synthesis at the micromole scale using 2- hydroxyethyl methacrylate grafted polyethylene supports. *Int. J. Peptide Protein Res.* **42**, 1–9.
13. Nicolás, E., Vilaseca, M. & Giralt, E. (1995) A study of the use of NH_4I for the reduction of methionine sulfoxide in peptides containing cysteine and cystine. *Tetrahedron* **51**, 5701–5710.
14. Brugidou, J., Legrand, C., Mery, J. & Rabie, A. (1995) The retro-inverso form of a homeobox-derived short peptide is rapidly internalised by cultured neurones: a new basis for an efficient intracellular delivery system. *Biochem. Biophys. Res. Commun.* **214**, 685–693.
15. Berlose, J.P., Convert, O., Derossi, D., Brunissen, A. & Chassaing, G. (1996) Conformational and associative behaviours of the third helix of Antennapedia homeodomain in membrane-mimetic environments. *Eur. J. Biochem.* **242**, 372–386.

UNITED STATES PATENT AND TRADEMARK OFFICE

CERTIFICATE OF CORRECTION

PATENT NO. : 5,888,762

DATED : March 30, 1999

INVENTOR(S): Alain JOLIOT et al.

It is certified that an error appears in the above-identified patent and that said Letters Patent is hereby corrected as shown below:

On the title page, item [30], the Foreign Application Priority Data should read:

--Jun. 5, 1990 [FR] France 90/06912--

Signed and Sealed this

Twenty-fourth Day of August, 1999

Attest:

Q. TODD DICKINSON

Attesting Officer

Acting Commissioner of Patents and Trademarks

UNITED STATES PATENT AND TRADEMARK OFFICE

Home | Index | Search | System Alerts | eBusiness Center | News & Notices | Contact Us

APPENDIX E

Trademark Electronic Search System(Tess)

TESS was last updated on Thu Aug 19 06:32:55 EDT 2004

PTO HOME | TRADEMARK | TESS HOME | NEW USER | FREE FORM | BROWSE DICT | BOTTOM | HELP

View Search History

WARNING: AFTER **SEARCHING** THE USPTO DATABASE, EVEN IF **YOU** THINK THE RESULTS ARE "O.K.," DO **NOT** ASSUME THAT YOUR MARK CAN BE REGISTERED AT THE USPTO. AFTER YOU FILE AN APPLICATION, THE USPTO MUST DO ITS OWN SEARCH AND OTHER REVIEW, AND MIGHT **REFUSE TO REGISTER** YOUR MARK.

Please enter search term in the fields below: **Records Returned:** 100 **Plurals:** Yes Quick Tips

Search Term	Field	Operator
"antennapedia peptide"	Goods & Services	AND
	ALL	

Submit Query | Clear Query

Logout *Please logout when you are done to release system resources allocated for you.*

PTO HOME | TRADEMARK | TESS HOME | NEW USER | FREE FORM | BROWSE DICT | TOP | HELP

HOME | INDEX | SEARCH | SYSTEM ALERTS | BUSINESS CENTER | NEWS&NOTICES | CONTACT US | PRIVACY STATEMENT